UMEÅ UNIVERSITY

Utilization of a GSHP System in a DHC Network

Modeling and Optimization

Anjan Rao Puttige

Department of Applied Physics and Electronics
Umeå 2021

Dissertation for PhD
ISBN: 978-91-7855-648-9(print)
ISBN: 978-91-7855-649-6 (pdf)
Electronic version available at: http://umu.diva-portal.org/
Printed by: Cityprint i Norr AB
Umeå, Sweden 2021

Table of Contents

Abstract ..... **iii**

Sammanfattning ..... **iv**

Preface ..... **v**

List of publications v

Additional publications not included in the thesis vi

Nomenclature ..... **vii**

1. Introduction **1**

Research objectives 3

Research flow and thesis outline 4

2. Background **7**

GSHP 7

BHE modeling 8

Heat pump modeling 10

ANN and its application in GSHP 12

Optimization of GSHP 14

3. Installation description **15**

BHE description 16

Heat pump description 17

Auxiliary components 17

Mode of operation 18

Measured data 19

4. Model description **20**

BHE model 20

Analytical model *20*

Calibration of Analytical model *21*

Hybrid BHE model *23*

Heat pump model 25

Individual models *25*

Combined model *27*

GSHP system model 28

5. Operation optimization **30**

6. Summary of results **32**

Models of GSHP using monitored data 32

BHE model *32*

Calibration of analytical model *32*

Hybrid BHE model *33*

Heat pump model *35*

Comparison of models *35*

Improvement of ANN model *37*

Combined model *38*

GSHP system model *38*
Operation optimization 40
7. Discussion 43
8. Conclusion 45
Acknowledgement 47
References 49

Abstract

The ground source heat pumps (GSHPs) of customers connected to the district heating and cooling (DHC) network can benefit both the customer and the energy company. However, operating the GSHP to minimize the cost of providing heating and cooling to the customer while ensuring the long-term stability of the ground temperature is a challenge. This thesis addresses the challenge by developing accurate models of GSHP and optimizing the operation of the GSHP system using these models.

The models presented in this thesis use field measurements to develop accurate models with low computational time. The main components of a GSHP system are the heat pump and the borehole heat exchanger (BHE). This thesis presents two approaches to use measured data to improve the accuracy of analytical models for BHE. The first approach is the calibration of the model parameters using this measured data. The second approach combines the analytical model with an artificial neural network model resulting in a hybrid model. The calibration approach reduced the relative RMSE of the analytical model from 21.9% to 13.9% in the testing period. The relative RMSE of the hybrid model for the testing period was 6.3%.

We compared different data-driven models for heat pumps and determined that artificial neural network models have an advantage over traditional regression models when field measurements are available. The artificial neural network model was refined to better utilize the measured data. The refined models of heat pumps had a relative RMSE of less than 5%.

The hybrid BHE model and an artificial neural network model for the heat pumps were used to model the GSHP system. The model was validated using four years of field measurements. The relative MAE for the compressor power and BHE power were 7.3% and 19.1% respectively.

The validated model was used to optimize the operation of the GSHP system. In optimal operation, the cost of providing heating and cooling to the area was minimized from the perspective of the energy company while maintaining a stable temperature in the ground. In optimal operation, the annual cost of operation was shown to reduce by 64 t€ and the annual CO_2 emission was shown to reduce by 92 tons.

Sammanfattning

Bergvärmepumpar som är anslutna till fjärrvärme- och kylnät kan vara till fördel både för användare och leverantörer av energi. I detta sammanhang utgör emellertid driftstrategin en stor utmaning för att minimera energikostnaden för att tillhandahålla värme och kyla och samtidigt säkerställa att marktemperaturen långsiktigt blir stabil. En viktig målsättning med denna avhandling har därför varit att förfina och utveckla modeller för driftoptimering av ett bergvärmepumpsystemi samverkan med ett fjärrvärmenät.

Huvudkomponenterna i ett bergvärmepumpsystem är värmepumpen och borrhålsvärmeväxlaren. Denna avhandling presenterar två metoder för att använda verkliga driftdata med syftet att förbättra noggrannheten hos analytiska modeller för borrhålsvärmeväxlaren. Det första tillvägagångssättet är kalibrering av modellparametrarna med hjälp av uppmätta data. Det andra tillvägagångssättet kombinerar den analytiska modellen med en artificiell neural nätverksmodell som resulterar i en hybridmodell. Kalibreringsmetoden reducerade den analytiska modellens standardavvikelse från 21,9% till 13,9% under testperioden. Standardavvikelsen för hybridmodellen för testperioden var 6,3%.

Vid jämförelsen av olika datadrivna modeller för värmepumpar konstaterades det att artificiella neurala nätverksmodeller har en fördel jämfört med traditionella regressionsmodeller då fältmätningar är tillgängliga. Den artificiella neurala nätverksmodellen förfinades för att på bästa sätt nyttja uppmätta data. Med de förfinade modellerna erhölls en standardavvikelse på mindre än 5%.

Borrhålsvärmeväxlarens modell och en artificiell neural modell för värmepumparna användes för att modellera bergvärmepumpsystemet. Modellen validerades med driftdata från fyra års fältmätningar. Det relativa medelfelet för kompressoreffekten och borrhålsvärmeväxlarens effekt var 7,8% respektive 19,1%.

Den validerade modellen användes för att optimera driften av bergvärmepumpsystemet. Vid optimal drift minimerades kostnaden för att tillhandahålla uppvärmning och kyla sett ur energileverantörens perspektiv, samtidigt som en stabil temperatur i marken bibehölls. Vid optimal drift visade sig den årliga driftskostnaden minska med 64 t€ och det årliga koldioxidutsläppet visade sig minska med 92 ton.

Preface

Heating and cooling play a significant role in the transition to a sustainable energy system. GSHPs can be an important part of the future energy system as they can efficiently use electricity to supply heating and cooling and store excess heat and cold for long periods. A connection between GSHP and the DHC network is desirable as it helps in the integration of the energy system.

This thesis explores how to operate a GSHP of a customer connected to DHC to make the production heating and cooling more economical and sustainable. The operation of a customer's GSHP is considered from the perspective of an energy company, thus alluding to the subject of prosumers. The main method used in this thesis is mathematical modeling, which has been used to simulate and improve the performance of the heating and cooling system. Methods to improve the accuracy of the model using field measurements were studied. We used a large GSHP at the University Hospital in Umeå that also subscribes to the DHC network as the case study in this work. The study was performed at the Department of Applied Physics and Electronics at Umeå University. This work was financially supported by the Industrial Doctoral School at Umeå University and Umeå Energi AB.

List of Publication

This thesis is based on the following papers, which are included in this thesis:

Paper I.	Improvement of Borehole Heat Exchanger Model Performance by Calibration Using Measured Data. **Puttige, A.R.** , Andersson, S., Östin, R., Olofsson, T. (2020) Journal of Building Performance Simulation, 13 (4), 430–42
Paper II.	A Novel Analytical-ANN Hybrid Model for Borehole Heat Exchanger. **Puttige, A.R.** , Andersson, S., Östin, R., Olofsson, T. (2020) Energies 13 (23), 6213
Paper III.	Application of Regression and ANN Models for Heat Pumps with Field Measurements. **Puttige, A.R.** , Andersson, S., Östin, R., Olofsson, T. (2021) Energies 14 (6), 1750
Paper IV.	Modeling and Optimization of Hybrid Ground Source Heat Pump with District Heating and Cooling. **Puttige, A.R.** , Andersson, S., Östin, R., Olofsson, T. (Under Review – Energy and Buildings)

Paper I presents a method to calibrate a simple analytical model using the measured data. The calibration improves the accuracy of the BHE model. Paper II presents a hybrid model for a BHE that tries to combine the long-term

prediction capability of an analytical model with the accuracy and computational efficiency of artificial neural network models. Paper III compares different data-driven models for modeling heat pumps and presents a method to refine artificial neural network models to better utilize the available data. Paper IV uses the hybrid model for borehole heat exchanger and an artificial neural network model for heat pumps to represent the whole GSHP and uses the model to optimize the operation of the GSHP.

Additional Publications not included in the thesis

Numerical Modeling of Ground Thermal Response with Borehole Heat Exchangers Connected in Parallel. Monzó, P., **Puttige A.R.**, Acuña, J., Mogensen P. ,Cazorla, A., Rodriguez, J., Montagud, C., Cerdeira, F. (2018), Energy and Buildings, 172, 371-384

Method to Estimate the Ground Loads for Missing Periods in a Monitored GSHP. **Puttige, A.R.**, Andersson, S., Östin, R., Olofsson, T. In European Geothermal Congress 2019 Den Haag, The Netherlands, June 11-14, 2019

Nomenclature

Symbols

x_t	Input of an RNN at time t
a_t	Activation of an RNN at time t
y_t	Output of an RNN at time t
$T_{b,i}$	Borehole wall temperature of borehole i (^oC)
$T_{fin,i}$	Inlet temperature of borehole i (^oC)
nb	Number of boreholes
r_b	Borehole radius (m)
H	Active length of borehole (m)
D	Groundwater level (m)
k	Thermal conductivity of the ground ($W(mK)^{-1}$)
ρC_p	Volumetric heat capacity of the ground ($MJK^{-1}m^{-3}$)
R_b	Borehole resistance (mKW^{-1})
T_{ug}	Undisturbed ground temperature (^oC)
$BHATb_{ana}$	Average borehole wall temperature of borehole group A from the analytical model (^oC)
$BHBTb_{ana}$	Average borehole wall temperature of borehole group B from the analytical model (^oC)
$BHAP_{ana}$	Average borehole power of borehole group A from the analytical model (W)
$BHBP_{ana}$	Average borehole power of borehole group B from the analytical model (W)
$BHATin_t$	Inlet temperature of borehole group A at time t (^oC)
$BHBTin_t$	Inlet temperature of borehole group B at time t (^oC)
$BHAmf_t$	Mass flow rate in borehole group A at time t (kgs^{-1})
$BHBmf_t$	Mass flow rate in borehole group B at time t (kgs^{-1})
$BHAP_t$	Power of borehole group A at time t(w)
$BHBP_t$	Power of borehole group B at time t (W)
N_{aa}	Number of hours after the last analytical step
T_C	Condenser temperature (^oC)
T_E	Evaporator temperature (^oC)
Q_c	Condenser power (W)
UT_r	Fraction of time the compressors are on
Q_{cr}	Ratio of actual condenser power to design condenser power
Q_{SC}	Sub-cooler power (W)
CompPower	Compressor power (W)

HPCoolmf	Mass flow rate of the cooling circuit (kgs^{-1})
HPHeatPower	Total Condenser Power of heat pumps (W)
HPHeatTout	Outlet temperature of heating side of heat pump (^oC)
DHWPower	Domestic hot water power (W)
DWHTout	Outlet temperature of domestic hot water (^oC)
HPCoolTin	Inlet temperature of cooling side of heat pump (^oC)
HPCoolPower	Evaporator power (W)
CoolTin	Outlet temperature of cooling side of heat pump (^oC)
BHP	Total power of the BHE (W)

Abbreviations

GSHP	Ground source heat pump
DHC	District heating and cooling
BHE	Borehole heat exchanger
RMSE	Root mean square error
MAE	Mean absolute error
ANN	Artificial neural network
TRT	Thermal response test
RO	Research objectives
RNN	Recurrent neural networks
LSTM	long short-term memory
GRU	Gated recursive units
HXH	Heat exchanger of heating circuit
HXC	Heat exchanger of cooling circuit
HXDHW	Heat exchanger for domestic hot water
3WVH	Three-way valve of heating circuit
3WVC	Three-way valve of cooling circuit
DHW	Domestic hot water
UPV	Universitat Politècnica de València
LM	Levenberg-Marquardt
COP	Coefficient of performance
HP1&2	Heat pumps 1 and 2
HP3	Heat pump 3
NN	Neural network
LMTD	Log mean temperature difference

1 Introduction

Space heating and cooling accounts for more than 25% of the total energy in Europe[1]. Despite the increase in the share of renewables recently, the percentage of renewable energy in heating and cooling is only 21%[2]. Hence, making heating and cooling more efficient and sustainable will increase energy security, cut costs for households and businesses, and help the EU in achieving its greenhouse gas emission reduction goals[3]. District heating and cooling (DHC) and heat pumps have the potential to increase the share of renewable energy[4,5] through the use of waste heat, biomass, and electrification. Moreover, DHC and heat pump help in the integration of the energy system[6]. An integrated energy system allows the transfer of energy among heat, cold and electrical networks. Heat pumps can play a crucial role in the integration by converting excess electricity to heat or cold, which can be easily stored for later use.

In Sweden, around 55% of the heating for residential and service sector buildings is supplied by district heating, and around 20% is supplied by heat pumps[7]. The high share of DHC and heat pumps has enabled Sweden to reach 65% renewable energy for total heating and cooling[2]. DHC is dominant in buildings with high demand density, like multi-family buildings and service sector buildings, where DHC has more than 80% market share. In single-family buildings, DHC is less dominant, with only a 17% market share[7]. Heat pumps are a common alternative to DHC in single-family houses. In recent years, due to increasing building efficiency and improvements in heat pumps, heat pumps are being used in multi-family and service sector buildings, especially ground source heat pumps (GSHPs). Hence, GSHP's are considered as a serious competitor for DHC[8,9]. This trend is expected to continue as the share of renewable electricity increases[10].

The overlap in the markets of GSHP and DHC has resulted in many buildings with both GSHP and DHC. If operated properly, such buildings can benefit both the energy companies and the building owners[11]. GSHPs connect the heating network to the electric network, which can increase the utilization of renewable energy and reduce costs[6,12,13]. However, there are a few concerns that have to be addressed for heating and cooling systems with both GSHP and DHC to operate beneficially. A non-optimal distribution of load between the GHSP and the DHC might increase the cost of the energy company and/or the building owner. An additional concern for the building owner is the long-term stability of the GSHP. The GSHP extracts and/or injects heat into the ground, which can accumulate over the years and change the temperature of the ground, which changes the efficiency of the GSHP.

Operating the GSHP to minimize the cost while maintaining long-term stability requires a reliable model of the GSHP. The main components of a GSHP are the heat pump and the borehole heat exchanger (BHE). In order to consider the long-term stability, the BHE model must consider a time scale of several years due to the large heat capacity of the ground[14]. The BHE model must also consider shorter time scales to simulate the energy performance of the heat pump accurately. The large variation in time scales makes the modeling of BHE hard, especially for large BHE.

The modeling of BHE is an active research area, but a model with a reasonable computational time that can represent both the long-term and short-term effects is still not available. Most models aim to be accurate in either the short-term or the long-term but not both. The long-term models use analytical[15–22] or numerical[23–27] methods to accurately represent the ground around the BHE but use a simplified representation of the inside of the BHE. The short-term models, on the other hand, use detailed numerical models[28–30], or a combination of resistor and capacitors[31–35], or analytical solutions[36–40] to represent the inside of the BHE and simplify the model of the ground. There have been some attempts to combine the long-term and short-term models[41–43]. The large computational time required for such models makes it impractical to use such models for the optimization of large GSHPs. In fact, most models for optimization of GSHP use a simple BHE model[44–48] or no BHE model[49,50].

Another issue with the modeling of BHE is the availability of accurate properties of the ground. The properties of the ground for larger BHE are usually determined through an in-situ thermal response test (TRT)[51,52], in which the temperature variation of the circulating fluid is used to determine the properties of the borehole and the ground. The properties obtained from TRT have a high uncertainty[53]. Moreover, the properties of the ground might vary due to ground water flow and ground water level.

With the increase in the number of larger GSHP, the number of monitored GSHP has also increased. As a result, the interest in methods to utilize monitored data has also increased. Several studies have used the monitored data for the validation of models[54–57]. More recently, the monitored data has been used to improve BHE models. The uncertainty in thermal properties of the BHE can be reduced through calibration using the monitored data[58,59]. There are also many examples of data-driven models for GSHP[60–64]. These examples show that the monitored data can be used to overcome the shortcomings of BHE models. However, more research is required to develop methods that can utilize the monitored data.

Data-driven models have been used for heat pump modeling. Several regression models can use the monitored data or data from the manufacturers to predict the performance of a heat pump[65–68]. More complex data-driven models like artificial neural networks (ANN) have also been used to represent heat pumps[69–71]. The accuracy of data-driven models also depends on the quantity and quality of data used to train the models. The accuracy of the models can deteriorate if the actual operating conditions are not reflected in the training data[72,73]. Therefore, a better understanding of the relationship between the data availability and the choice of model is required.

1.1 Research Objectives

The overarching objective of this thesis is to develop a method to optimize the operation of a customer's GSHP that operates in parallel to a DHC network. The objective of the optimization is to reduce the cost of producing the energy for heating and cooling while ensuring the sustainable operation of the GSHP. To achieve this objective, we needed an accurate model of GSHP that is computationally efficient. Therefore, the other objective of this thesis is to develop models of a GSHP and its components that use monitored data to have high accuracy while keeping the computational time low. The specific research objectives (RO) of this thesis are:

RO1: Develop an accurate model for a GSHP using monitored data

RO2: Develop a model for a BHE that uses monitored data to improve the accuracy of the model and is computationally efficient

RO3: Develop an accurate model for a heat pump using monitored data

RO4: Optimize the operation of a consumer's GSHP operating in parallel to a DHC network

Through these research objectives, the thesis attempts to contribute to the field of modeling and optimization of GSHP. The methods developed in this thesis are used to demonstrate the benefits of operating a customer's GSHP in cooperation with the DHC network operator. However, the models and the optimization method developed in this thesis have a broader field of application. Developing a good BHE model that can consider both short-term and long-term effects is still an open problem. This thesis contributes towards a solution to this problem. The models developed in this thesis also show how to utilize the increasing amount of data from field measurements to improve model predictions. The model predictions can be used to improve the performance or to detect faults of GSHP systems. The optimization method developed in this thesis presents a way to

consider and compensate for the effect of the long-term operation of GSHP while developing a control strategy. This method can be used in many GSHP applications, with multiple heating and/or cooling sources.

1.2 Research flow and thesis outline

The research objectives of the thesis were addressed in four research papers published/submitted during the Ph.D. The objectives RO2 and RO3 were addressed first so that RO1 could be achieved. The first two papers attempted to achieve RO2, i.e., the development of a model for a BHE that uses monitored data to improve the accuracy of the model while keeping the computational time low. Paper II and I present two different approaches to achieve RO2. In Paper I, the measured data was used for improving the accuracy of a simple analytical model through calibration. Paper II presented a hybrid analytical ANN model for BHE. After comparing the two approaches, the hybrid approach was adopted for the final model of GSHP. Since data-driven models are already prevalent in the modeling of heat pumps, Paper III achieved RO3 by addressing the challenge of choosing and refining data-driven models of heat pumps to best suit the available data. A model of an entire GSHP was presented in Paper IV, hence completing RO1. Paper IV also presented a method to optimize the operation of a GSHP operating with DHC to satisfy the heating and cooling needs of an area using the model of GSHP, i.e., RO4 was also accomplished. Figure 1 shows the flow of research and the research objective/s of each paper of the thesis.

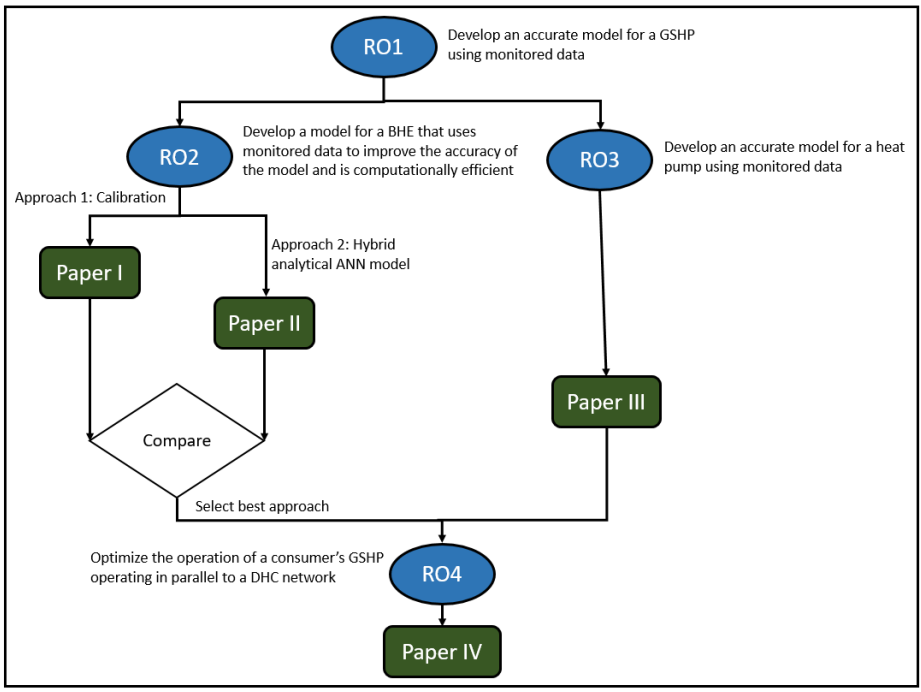

Figure 1: Flow of research in the thesis showing the research objectives and the research articles addressing the research objectives

This thesis is organized into eight chapters, Introduction, Background, Installation Description, Model Description, Operation Optimization, Results, Discussion, and Conclusion.

Chapter 1 provides the overall context of the thesis and introduces the research objectives. Chapter 2 summarizes earlier works in the field to provide the context of the current work. The methods in this thesis were developed using the case study of a hospital area in northern Sweden. The hospital has a large GSHP, which is used along with the DHC network to meet the heating and cooling demands of the buildings. A description of the heating and cooling system with a focus on the GSHP system is presented in Chapter 3. Chapters 4 and 5 describe the methods used in the thesis. Chapter 4 presents the models developed in this thesis. The first part of the chapter presents models for the BHE. The measured data is used to improve an analytical model presented in Chapter 4.1.1. The calibration method from Paper I is described in chapter 4.1.2, and the hybrid model from Paper II is described in chapter 4.1.3. The models for heat pumps used to achieve RO3 are presented in Chapter 4.2. Chapter 4.3 describes the model of the complete GSHP system. The optimization method used to achieve RO4 is presented in chapter 5. The summary of the results of methods in chapter 4 and

chapter 5 is presented in chapter 6. A discussion about the results and the future direction of the research is presented in chapter 7. The main conclusions of the thesis are summarized in chapter 8.

2 Background

2.1 GSHP

Heat pumps transfer heat from a low-temperature to a high-temperature heat source. The efficiency of heat pumps is inversely proportional to the temperature difference between the sources. Due to the relative stability of the ground temperature, the ground is at a higher temperature than the outdoor air in winter and lower temperature than the outdoor air in summer. GSHP uses this to increase the efficiency of heat pumps. (Note: the term ground source heat pump (GSHP) is used in this thesis, even though the ground can be used as both heat source and heat sink) The heat can be extracted from/injected into the ground using open-loop or closed-loop systems. Open-loop systems directly use groundwater as heat source/sink, while closed-loop systems extract/inject the heat from the ground using a secondary fluid through a heat exchanger. Closed-loop systems dominate the market due to strict regulations regarding the use of groundwater and issues related to water quality[8,74]. Closed-loop systems can have either horizontal or vertical heat exchangers. Vertical heat exchangers have a higher installation cost, but they are more efficient and require lesser land[25,74,75]. Hence, vertical heat exchangers are the most common type of BHE, especially for larger installations[25,76].

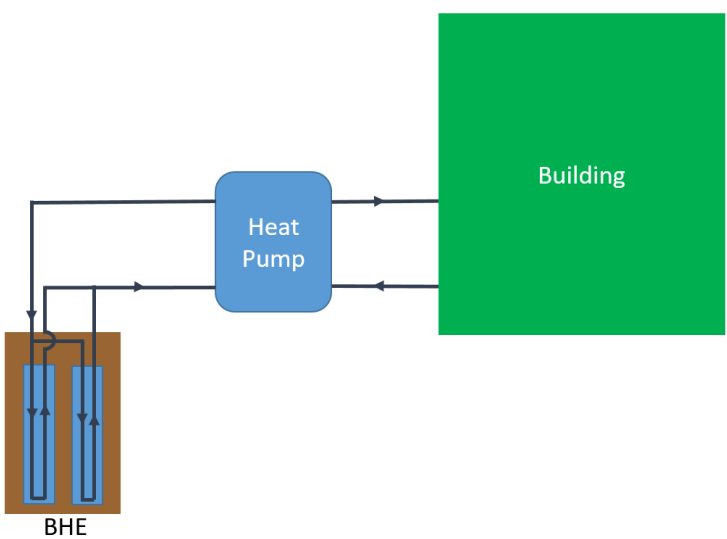

Figure 2: Schematic of the main components of a GSHP with closed-loop vertical BHE

Figure 2 shows a schematic of a GSHP with closed-loop vertical BHE. A GSHP consists of a ground circuit that extracts/injects heat into the ground, a building circuit that delivers the heat/cold to the buildings, and a heat pump. GSHPs were first commercially used in the 1940s. Since then, the use of GSHP has grown whenever there was a need for increased energy efficiency [76]. Sweden has a long history of GSHP use, with initial development in the 1970's and rapid development in the '80s and '90s, during which period Sweden became the world leader in GSHP research and industry[8]. Historically, single-family buildings have been the primary market of GSHPs, but in the last decade, the market of larger GSHPs also has increases[8]. Larger GSHPs are often used for both heating and cooling. Hence the ground acts as a storage for heat and cold.

The ability of GSHP to store energy can increase the utilization of waste heat[77,78] and solar energy[79]. The connection of GSHPs with the electrical network helps in the utilization of surplus electricity[12] and increases the utilization of renewable electricity[13]. Therefore, GSHP can play an important role in future energy systems as a connection between electrical and DHC networks and as a store of excess energy in the energy system.

2.2 BHE modeling

Most BHE models can be classified into long-term models and short-term models. Long-term models focus on modeling the heat transfer in the ground around the borehole, also called the global problem, while short-term models focus on modeling the heat transfer inside the borehole. Due to the relatively low heat capacity of the borehole, the heat transfer inside the borehole is only important for time scales of a few hours. For time scales of a few hours to decades, the heat transfer in the ground is important[14].

Eskilson[23] proposed the use of a response function of a BHE, called the g-function, to simplify the long-term models. The g-function is the non-dimensional temperature response of a BHE to a constant heat load. The response of the BHE to a variable load can be obtained using temporal superposition. Eskilson presented a finite difference method and an analytical method that represents the borehole as a finite line source (FLS) to calculate the g-function. Since then, several numerical and analytical methods to calculate the g-function have been proposed.

Finite difference method has a more accurate representation of the boundary condition at the borehole wall compared to the finite line source method. This leads to a more accurate g-function of the BHE, especially when there are multiple boreholes with high interaction[80,81]. Hence, numerical methods are used in many commercial software like earth energy designer[82] and GHLEPRO[83].

The numerical models for BHE have been improved further by using a more accurate representation of the boundary condition at the borehole wall [26,80,84], considering groundwater flow[85,86], and considering heterogeneous soil[86,87]. Despite the improvements, the main disadvantage of the use of numerical models for large BHE is their computational time. Due to the high computational time, numerical models are generally used for a limited number of geometries, for which the g-functions are pre-computed and stored[88].

Analytical models have lower computational times; hence they can be calculated in the model. Therefore, the geometry of the BHE is not restricted by pre-calculated g-functions. Most of the analytical models are based on the FLS approach, where the borehole wall is represented by a line source of finite length, and an adiabatic boundary condition is applied at the top surface of the ground[15,23]. Lamarche and Beauchamp[89] and Marcotte and Pasquier[18] reduced the computational time for the FLS method using Laplace and Fourier transform, respectively. Lamarche[17] introduced the non-history scheme, which aggregates all the previous loads, hence making it easy to simulate hourly loads. The inaccuracy in the boundary condition at the borehole wall was corrected by first using different heat flux for each borehole[81,90] and then by using different heat flux for different segments of a borehole[19]. Therefore, overcoming the main disadvantage of analytical models. The range of BHE configurations that can be simulated was increased using models that can simulate BHE with multiple inlets[20,90–92]. Lazzarotto[93] introduced a model that can include boreholes with different inclinations. Analytical models that can consider geothermal gradient[21], multi-layered ground[94], and groundwater flow[22] have also been presented.

Numerical and analytical approaches have also been used for short-time models. Many numerical models based on finite difference method and finite element method with different levels of details have been used for short-time models[28–30,95]. The analytical models use different approaches to solve the heat transfer problem inside the borehole. The most common approach is to represent the borehole as a network of resistors and capacitors. Capacitance resistance model (CaRM)[32], thermal resistance-capacitance model (TRCM)[33,96], and borehole to ground (B2G) model[35,97] are all examples of this approach. Javed and Claesson[34] represented the borehole as a thermal network in the Laplace domain. Another approach is to model each leg of the BH as an infinite line source in a composite medium as presented in[38] and simplified by using a single line with equivalent diameter in[98]. The idea of representing the different legs of the BH as a single pipe of the equivalent radius is used in many models as this simplifies both numerical and analytical solutions. Xu and Spitler[99] and Naldi and Zanchini[29] used this approach to simplify numerical models of the BH.

Several researchers[16,36,37] used the single pipe of equivalent radius approach to finding exact analytical solutions to the heat transfer problem. Recently Rivero and Hermanns[39] and Prieto and Cimmino[40] presented transient multipole method to solve the two-dimensional heat transfer problem inside the borehole without simplifying the geometry of the borehole.

All the above short-term models consider that the boreholes are grouted, which is often not the case in Scandinavia, where boreholes are naturally filled by groundwater instead. Most models handle natural convection in groundwater-filled boreholes by assuming an effective thermal conductivity for water. But several studies have shown that natural convection depends on temperature [100][101][102]. Hence using a single value for all the conditions is not accurate. Spitler et al.[103] presented a correlation between natural convection in the annulus and modified the Rayleigh number based on experimental measurements to address this issue. However, the authors commented that the correlation is not accurate and Johnsson and Adl-Zarrabi[104] demonstrated it in their study. Therefore, developing an accurate short-term model for groundwater-filled boreholes is still an open problem

Short-term models can be combined with long-term models by either combining the g-functions obtained from the two models or by coupling the two models using the conditions at the borehole wall. In the first approach, the g-function obtained from the short-term model is used for time scales below a threshold, and the g-function from the long-term model is used for time scales above the threshold[14,28]. The second approach can either be implemented by a complete coupling of the two models[105–107], which is possible if both are numerical models, or by using the solutions of the long-term model as the boundary condition for the short-term model[42].

2.3 Heat Pump Modeling

Heat pump models can be divided into four groups[108]

- Balanced energy approach: In this approach, the overall efficiency for the whole year is calculated using a few standard operating points.
- Steady-state models: These models use component-level steady-state modeling to represent the heat pumps. The models are based on the thermodynamic properties of the refrigerant and the efficiencies of the components.
- Regression models: They use manufacturer or field data to fit performance parameters to operating conditions like evaporator and condenser temperature.

- Dynamic models: They are detailed models that consider the transient behavior of the heat pump.

Dynamic models[109–111] consider the transient properties of a heat pump. The transients in a heat pump are much faster than the transients in the BHE or the buildings. The transient considerations are only important for time scales of less than a few minutes[108]. The balanced energy approach evaluates only the seasonal or annual efficiency of heat pumps. Steady-state models and regression models are suitable to evaluate the long-term hourly performance of a heat pump.

Steady-state models[112,113] use simplified refrigeration cycles and the efficiencies of the components to obtain performance parameters like the compressor power and COP. The steady-state models require the properties of the refrigerants and the performance parameters of the components. The performance parameters of the components are obtained by calibrating the model using experimental data or data provided by the manufacturer[113,114]. The assumptions and the uncertainty in the parameters limit the accuracy of steady-state models.

Regression models map the performance of heat pumps (COP/ compressor power) to operating conditions, like condenser temperature, evaporator temperature, condenser power, etc. The coefficients of the regression models are obtained by fitting the models to performance data provided by the manufacturers or measured in experimental or actual operation. Regression models with different levels of complexity have been used, the bilinear model [108] is the simplest model, and ANN models [70,115] are one of the most complex models used in literature. Second-degree polynomials are the most common form used in regression models [66,67,116]. Regression models are more accurate than steady-state models within the range of the training data[73,108]. The main advantage of steady-state models over regression models is that they have better performance outside the range of the training data. Therefore, when a large amount of data from the actual operation of the heat pump is available, regression models are a better choice.

Several studies have compared the performance of regression models. Lee and Lu[68] compared the performance of 6 models using laboratory and field measurements from over 1000 heat pumps. They found that the bi-quadratic model to be the best among the models. Swider [69] compared six models, including two ANN models using experimental data from two heat pumps. The ANN models were found to have better performance than other regression models. Ruschenburg[117] compared the performance of a biquadratic model with a modified quadratic model using field measurements from 5 installations. The modified model used a biquadratic model for the interpolation and a linear

model for extrapolation. They found that the modified model had a better performance than the biquadratic model, but the error in predicting field measurements was up to 13%. The deterioration of model performance while predicting field measurements was also highlighted by Zhang et al. [72]. They compared 13 regression models and found that all the models fit the manufacturer's data well, but when the models were used to predict the performance of a building, the results from the models had a maximum deviation of around 30%.

2.4 ANN and their application in GSHP

ANNs are black-box models, i.e., they do not require any knowledge of the physical system, that tries to mimic the structure of the brain to identify patterns between inputs and outputs. ANNs use a large number of interconnected processing units, called nodes, arranged in layers[118]. Figure 3 shows the structure of a fully connected ANN, in which each node is connected to all the nodes of the previous layer. A fully connected ANN consists of an input layer, an output layer, and one or more hidden layers. Figure 3 represents the processing inside a node. The weighted sum of all the inputs to the nodes is transformed using a non-linear activation function to calculate the output of the node. The weights of the ANN are calculated by training the ANN using training data. ANNs with a sufficient number of nodes can approximate any continuous function.

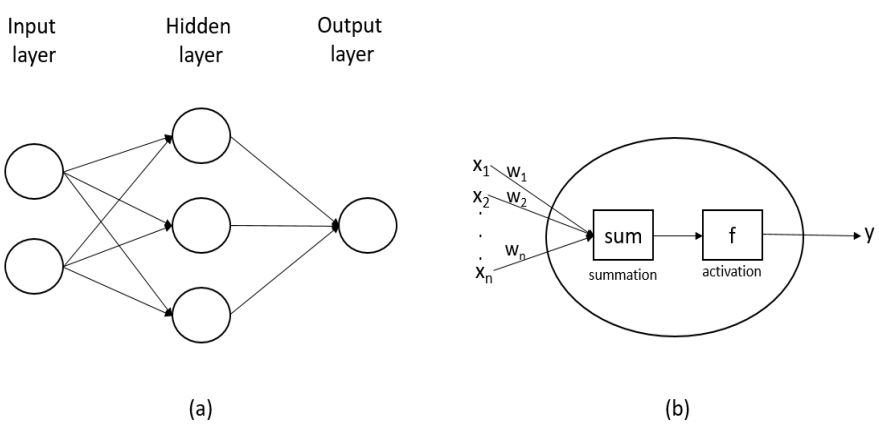

Figure 3: Schematic of (a) an ANN network (b) a single node of an ANN (adopted from Paper III)

The outputs of an ANN are calculated based on the inputs. Hence, if the output depends on a sequence of inputs, the entire sequence of inputs must be used as inputs to the ANN. For example, in the case of a BHE, the entire thermal history of the BHE must be used as input to calculate the temperature response of the

BHE. This implies that the number of inputs should increase as time increases. Recurrent neural networks (RNN) are a class of artificial neural networks that pass the information from one step to the next to solve this issue. Figure 4 shows the architecture of an RNN. At each step, the inputs (x_t) and activation from the previous step (a_{t-1}) are used to calculate the activation of the current step (a_t), which in turn is used to calculate the output (y_t). The activation acts as a memory to remember the previous inputs. The ability of inputs to influence future outputs is limited in an RNN due to vanishing gradients. Therefore, long short-term memory (LSTM)[119] and gated recursive units (GRU)[120] were developed to retain useful information for a longer time.

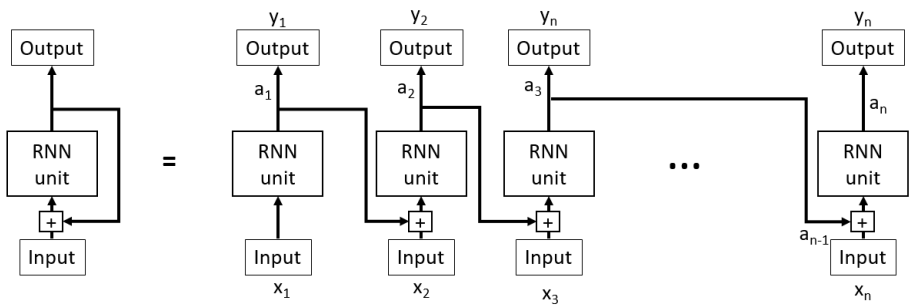

Figure 4: Schematic of an RNN (adopted from Paper II)

The advances in artificial intelligence and increase in the amount of data in the past decades have led to an explosion in the application of ANN and other machine learning techniques in many fields, including heating and cooling[118,121,122]. Esen et al.[123] presented one of the earliest applications of ANN in GSHP. They predicted the COP of a GSHP using the inlet and outlet temperatures of the condenser and the ground temperature as the input. Esen and Inalli[60] presented a similar model for vertical BHE. Other studies[61,124,125] have used a similar approach of predicting the overall performance of the GSHP instead of using separate models for BHE.

Chen et al.[126] developed an ANN model to determine the depth of a borehole using the hydrothermal properties of the ground and the design operating conditions as the input parameters. Arat and Arslan[127] presented an approach to optimize a GSHP for district heating using ANN. ANN has also been used to predict the properties of the ground using geological data[128,129]. Pasquier et al.[62] presented an ANN model to generate short-term g-function and Dusseault and Pasquier[130] presented a model for long-term g-function. Gang and Wang[63] and Lee et al.[64] presented ANN models of BHE for control of GSHP. Both the studies used numerical models to train the ANN.

2.5 Optimization of GSHP

Optimizing the operation of a GSHP can reduce the economic and environmental cost of providing heating and/or cooling, especially when there are multiple sources of heat. However, due to the complexity of modeling of BHE, most attempts to optimize the operation of GSHP use simplified models. Sayyadi and Nejatolahi[131] used the genetic algorithm to optimize the operating parameters of a cooling tower-assisted GSHP, but they considered the temperature of the ground as a constant. Ikeda et al.[46] optimized the load distribution between GSHPs, air source heat pump, and auxiliary boiler for periods of one day and one week. They used an infinite line source model, which does not consider the short-term response of a BHE. Sivasakthivel et al.[132] used experiments based on the Taguchi method to determine the dependence of GSHP performance on the operating parameters and used it to determine the optimal operating parameters.

Optimizing the operation of a GSHP in the design phase can reduce both investment and operation costs. However, the number of parameters to optimize is higher in such cases. Therefore, the importance of using simple models is also higher. Many studies use a constant ground temperature or a constant COP for the GSHP to optimize GSHPs operating with combined cooling and heating plant[50,133], solar photovoltaic[133], biomass heat, and power plants[49]. Miglani et al.[45] represented the ground using a long-term finite line source model and the heat pump using an empirical model to optimize the design and operation of a system with GSHP, solar photovoltaic, and solar thermal. Despite the simplified model, they did not consider loads of the whole year for optimization; instead, they used loads for seven representative days. Nouri et al. [48]and Reda[47] optimized the design and operation of solar-assisted ground source heat pumps in TRNSYS, but they only considered a limited number of configurations.

Detailed models of GSHP that consider short-term and long-term effects of the BHE are complex and computationally intensive. Hence, there are a limited number of examples of such models. Li et al.[134]presented a GSHP with a detailed numerical model for BHE with 15 boreholes and a regression model for the heat pump. They showed that increasing the imbalance of the load by reducing the heat load would reduce the long-term efficiency of the system. Ruiz-Calvo et al. [135] presented a GSHP model in TRNSYS with a BHE model that considers both short-term and long-term models for BHE[42]. However, these models were not used for optimizing the operation of GSHP. Figueroa[43] et al. presented a methodology to optimize the long-term operation of a hybrid GSHP using a model predictive control approach. However, the approach was applied to a simplified case.

3 Installation description

In this thesis, the heating system of the University Hospital buildings in Umeå, Sweden, was used as the case study to demonstrate the methods and achieve the research objectives. The GSHP system was installed in the hospital in 2016 as a supplement to the heat and cold from the district heating and cooling network. The GSHP is the primary source of cooling, which supplies around 92% of the load. The DH network provides the majority of the heating, and the GSHP provides only 15% of the load. Figure 5 (a) and (b) show the heating and cooling load of the heating system, respectively. The GSHP system can provide cooling to all the buildings at the hospital, but it can only provide heating to 2 buildings due to differences in temperature requirements among the buildings. The heat demand of the two buildings represents around 30% of the total heat demand.

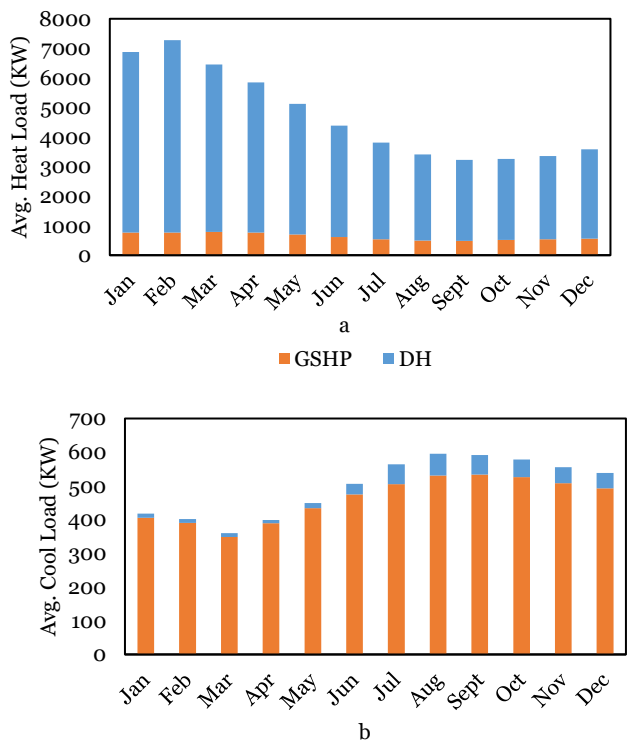

Figure 5: (a) Heating and (b) Cooling load of the GSHP and DHC network for the hospital area

The GSHP system is the focus of this thesis. Hence a description of the GSHP system and the data collected through motoring of the GSHP is presented in this Chapter. Figure 6 shows a schematic of the GSHP system. The main components

of the GSHP are a BHE divided into two groups and three heat pumps. The GSHP system also consists of some auxiliary components like heat exchangers and circulation pumps.

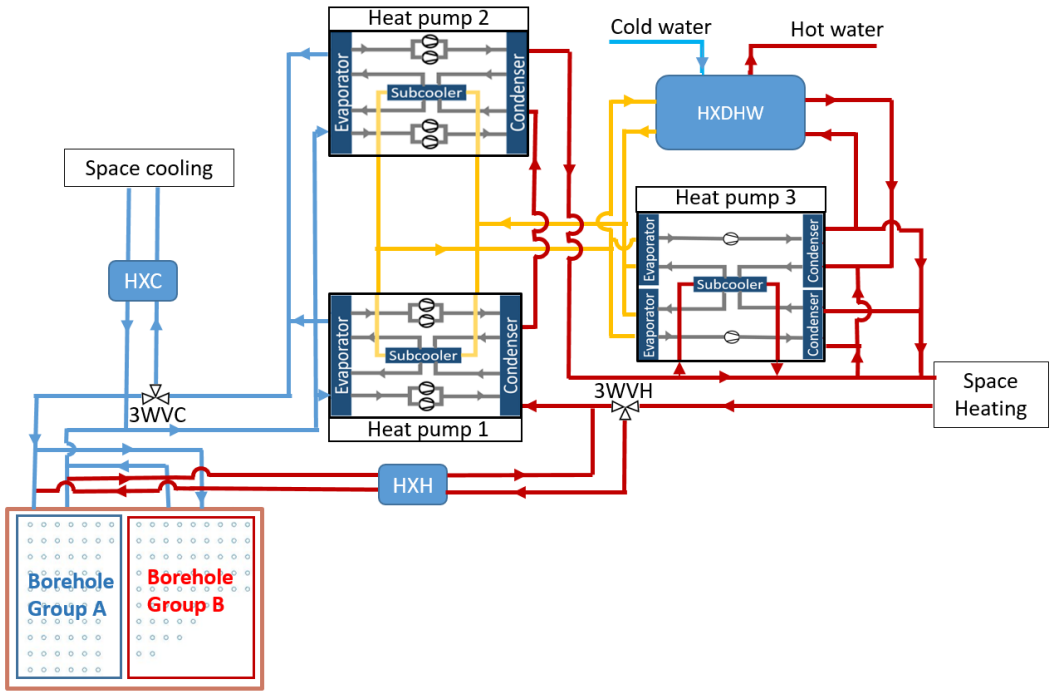

Figure 6: Schematic of the GSHP system at the University Hospital in Umeå

3.1 BHE description

In winter, the BHE acts as a source of heat for the heat pump, and in summer, the BHE provides free cooling and acts as a sink to the excess heat produced by the heat pump. The BHE is divided into two borehole groups with independent fluid loops to enable the dual function of the BHE in the summer. Each of the borehole groups can be connected to either the cooling circuit or the heating circuit. When connected to the cooling circuit, the BHE is used as a heat source or for free cooling, and when connected to the heating circuit through HXH, the BHE acts as a heat sink. Borehole group A consists of 62 boreholes with a diameter of 14 cm and a depth of 200 m. Borehole group B consists of 63 boreholes with a diameter of 14 cm and a depth of 250 m. The boreholes are arranged as shown in Figure 6, with a distance of 7 m between them. The boreholes have a single U-tube configuration. The boreholes are filled naturally with groundwater, with a groundwater level of 10 m. The properties of the ground and the borehole

resistance for injection were determined by an in-situ TRT. The properties of the ground and a further description of the BHE can be found in Paper I.

3.2 Heat pump description

The GSHP system consists of 3 heat pumps. Heat pumps 1 and 2 are the same model of heat pump, EMA from the manufacturer EnergyMachines. The evaporators of heat pumps 1 and 2 are connected in parallel and provide cooling. The condensers of heat pumps 1 and 2 are connected in series to provide heating. Heat pumps 1 and 2 have two circuits and four compressors each, two in each circuit. Hence, each of the two heat pumps can operate at 0%, 25%, 50%, 75%, and 100% capacity. The heat pumps also have a sub-cooler, which is used as a heat source for heat pump 3 and as a preheater for domestic hot water. Heat pump 3 uses the sub-coolers of heat pumps 1 and 2 as a heat source and provides heat for DHW and heating for the coldest days. Heat pump 3 also has two circuits but only one compressor in each circuit. The evaporators and condensers of heat pump 3 are not connected. Hence the two circuits can be considered as separate units.

3.3 Auxiliary components

The GSHP consists of three heat exchangers, HXC, HXH, and HXDHW. The HXC transfers the cooling from the heat pump to the cooling circuit of the buildings. The HXH transfers excess heat in the heating circuit to the BHE. The HXDHW has three heat exchangers, two of which pre-heat the cold water using the heat from the sub-coolers of heat pumps 1 and 2 and the third heat exchanger transfers heat from heat pump 3 to the preheated water to produce DHW.

The GSHP system also consists of circulation pumps for the cooling circuit, heating circuit, and BHE. Each of the heat pumps has a variable speed circulation pump for the heating and cooling circuits. The speed of the circulation pumps is determined based on the number of compressors operating in the heat pump. Borehole groups A and B each have a variable speed circulation pump. When a borehole group is connected to the cooling circuit, the circulation pump is controlled to minimize the flow through a bypass pipe for the BHE. When a borehole group is connected to the heating circuit, the circulation pump is controlled such that a set temperature is maintained at the outlet of the heat exchanger, HXH.

3.4 Modes of Operation

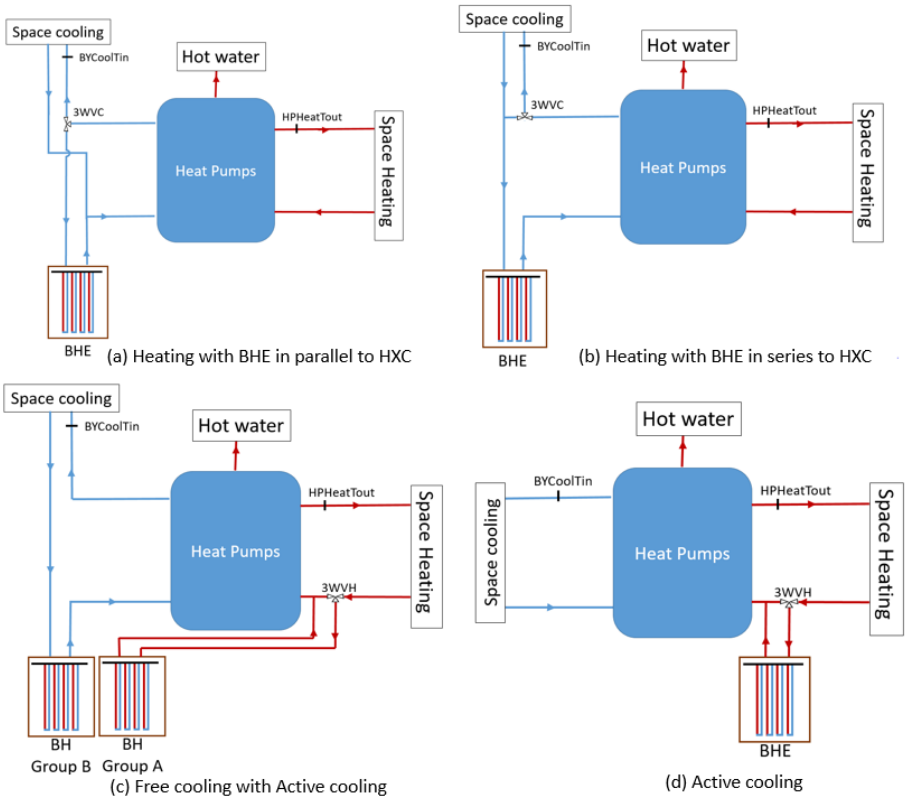

Figure 7: Simplified schematic of the four modes of operation of the GSHP

The GSHP system has four modes of operation based on the BHE's connection to the system. Figure 7 shows a simplified schematic of the four modes of operation, (a) heating with BHE in parallel to HXC, (b) heating with BHE in series to HXC, (c) free cooling with active cooling, and (d) active cooling. In winter, the GSHP operates in heating with BHE in parallel to HXC mode. In this mode, the heat pumps operate to satisfy the heating need, and cooling is a by-product. 3WVC directs the cooling required by the building to HXC, and the excess cool is extracted by the ground through the BHE. As the cooling load increases in the spring, the GSHP changes to heating with BHE in series to HXC. In this mode, the heat pumps are still controlled to satisfy the heating needs, but the BHE can be a heat source or provide free cooling. A part of the inlet flow to the BHE comes from the outlet flow HXC while the other part comes directly from the evaporator. If the temperature at the inlet of the BHE is greater than the ground temperature (typically 8 ^{o}C), the BHE provides free cooling. In summer, when the demand is cooling-dominated, the GSHP operates in free cooling with active cooling mode

or only active mode. In free cooling with active cooling mode, borehole group B is connected to the cooling circuit in series to HXC to provide free cooling, while borehole group A is connected to the heating circuit, and the excess heat from the heat pumps is injected into the ground. When all of the excess heat cannot be injected into borehole group A alone, the mode changes to only active cooling, in which both borehole groups are connected to the heating circuit to inject the excess heat into the ground. The transition of GSHP mode from heating with BHE in parallel to active cooling as the cooling load increases and vice versa when the heating load increases is represented in Figure 8. A detailed description of the operation of the GSHP can be found in Paper IV

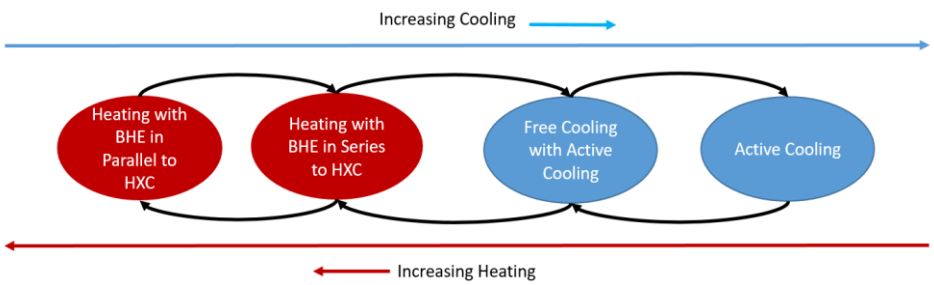

Figure 8: Illustration of change of modes of the GSHP with a change of heating and cooling loads (Adopted from Paper IV)

3.5 Measured data

The GSHP has been operational since February 2016. Some of the data, including the inlet and outlet temperature of the BHE, were measured from the start of the operation. A monitoring system for the entire GSHP was installed in January 2017, but the flow and energy meters for each of the two borehole groups were installed in March 2017. Hence, the complete measured data of the GSHP is available from March 2017 to the present day.

The measured data has many periods of missing or faulty data. Only periods of non-faulty data have been used to study the heat pumps and other auxiliary components, but to study the BHE, the ground loads for the entire period of operation are required due to the dependence of the performance of the BHE on historical loads of the ground. The mass flow rate in the BHE is not measured until March 2017, hence for the period from February 2016 to March 2017, the mass flow rate of the BHE was estimated using the power of the circulation pumps, as described in Paper I. In periods of gaps in the measured data, the ground loads were estimated based on the ambient temperature.

4 Model Description

Models for the components of the GSHP and a complete GSHP were developed in this thesis to achieve RO1. The models developed in this thesis focus on the utilization of data from the actual operation of the GSHP system. We demonstrated that data from the real operation of a GSHP could be used to develop models that are accurate with reasonable computational time, hence overcoming the limitations of traditional GSHP models. Multiple years of operational data of the GSHP system described in the previous chapter were used to develop and validate the models.

To achieve RO2, two models for the BHE that use the monitored data were developed in this thesis, as described in section 4.1. Accurate models of the heat pump that use the monitored data (RO3) are described in section 4.2. The BHE and heat pump models were used to achieve RO1, i.e., make a model for the whole GSHP system, as described in section 4.3.

4.1 BHE model

Developing a BHE model that can represent both the short-term and long-term response of the BHE accurately is a challenge. In this section, we present two ways to use the field measurements to improve the accuracy of BHE models based on an analytical model. The analytical model used in this thesis is presented in section 4.1.1. A method to calibrate the analytical model, based on Paper I, is described in section 4.1.2. In Paper II, a hybrid analytical ANN model was developed, as described in section 4.1.3.

4.1.1 Analytical model

An analytical model of the BHE was developed based on the model presented by Lamarche[20]. An analytical model was chosen as they have lower computational time compared to numerical models. The large computational time makes numerical models unsuitable for large borehole fields, like the one described in Chapter 3. The borehole field has two hydraulic loops that have different inlet temperatures during parts of the year. The model by Lamarche[20] was chosen for this work since it is one of the few analytical models that can represent a borehole field with multiple inlets.

The model represents the boreholes as finite line sources. The finite line source approach assumes a constant load. Hence Lamarche [17] proposed a non-history scheme to calculate the effect of a time-varying load. The inside of the borehole is represented by a single equivalent resistor in the model. At every time step, the

borehole wall temperature (T_b) of each borehole i was calculated using equation 1:

$$T_{b,i} = S_{p,i} + \sum_{j=1}^{nb} S_{q,ij} X_j \left(T_{fin,j} - T_{b,j}\right) \quad (1)$$

Where the first term $S_{p,i}$ accounts for the effect of historical load on borehole i, and the second term accounts for the effect of the current load. $S_{p,i}$ is updated at every step to include the effect of the previous step into the effect of historical load. $S_{q,ij}$ is the temperature response of the borehole i to a load in borehole j. X_j is a coefficient to convert heat load to temperature, and $T_{fin,j}$ is the inlet temperature of borehole j.

The equations for all the T_b were arranged in the form of a matrix equation, equation 2, and solved in MATLAB. The heat load and outlet temperature of the fluid were calculated using T_b and T_{fin}.

$$A \times T_b = B \quad (2)$$

4.1.2 Calibration of the analytical model

The geometrical attributes of the BHE and the thermal properties of the ground are the parameters of the BHE model. The parameter values used in the model are listed in Table 1. The geometry of the BHE was obtained from accurate design and drilling drawings. The thermal properties of the ground, i.e., k, ρCp, R_b, and T_{ug}, were determined using a TRT, which is known to have high uncertainty[53]. The uncertainty in the model parameter values, in particular the thermal parameter, affects the performance of the BHE model. Therefore, in this thesis, we used the measured data to calibrate the thermal parameters of the model to improve the performance of the BHE model.

Table 1: Parameters of the BHE (Adopted from Paper I)

	Parameter	**Value**
Geometry	Borehole radius (r_b)	0.070 m
	Borehole depth (H+D)	200 m/250 m
	Groundwater level (D)	10 m
Thermal	Thermal conductivity of the ground (k)	3.4 $W(mK)^{-1}$
	Volumetric heat capacity of the ground (ρCp)	2.3 $MJK^{-1}m^{-3}$
	Borehole resistance (R_b)	0.08 mKW^{-1} (0.11 mKW^{-1} for extraction)
	Undisturbed ground temperature (T_{ug})	5.9°C

The thermal parameters were estimated to minimize the squared deviation between the measured and predicted loads of the BHE. The model was calibrated using one year of measured data, from March 2017 to March 2018. A model-independent optimization program called GenOpt [136] was used for the minimization. A hybrid optimization algorithm, particle swarm algorithm followed by Hooke-Jeeves generalized search algorithm was used to find the global minima.

The parameters obtained from calibration are not accurate values of the thermal properties of the ground because the model used for calibration is not perfect. Hence, the calibrated parameter values not only compensate for the inaccuracy in the thermal properties but also for simplifications in the model. A number of factors affect the validity of the assumptions of the model, including the time resolution of the data, the season of measured data, and the number of years the BHE has been operational.

The model uses a simplified, single equivalent thermal resistor model to represent the inside of the borehole. Hence it is not accurate in the short time scale. The model also ignores the variation of heat flux in the vertical direction, which makes it less accurate in large time scales. Therefore, changing the time resolution of the model in the calibration period can affect the values of the calibrated parameters. Hence, it can influence the accuracy of the calibrated model. Therefore, we calibrated the parameters using three different time resolutions, 30-day, 1-day, and 6-hour, and tested each of the calibrated parameter values to simulate the BHE at four different time resolutions, 30-day, 1-day, 6-hour, and 1-hour.

The properties of the ground are affected by the weather; for example, groundwater flow and groundwater level can affect the properties of the ground. Moreover, in groundwater-filled boreholes, the temperature and load of the BHE affect R_b, both of which change with the season. Therefore, we divided the calibration data into six seasons, four 4-month long periods, corresponding to the seasons, winter, spring, summer, and fall, and injection period when heat is injected into the ground and extraction period when heat is extracted from the ground. We tested if using different parameters for different seasons improves the accuracy of the model.

The analytical model does not consider the axial variation of heat flux in the borehole, due to which the interaction between the borehole is underestimated in the long term (in the time scale of years)[137]. Re-calibrating the model at regular intervals can reduce the effect of this assumption. We used a 2×3 BHE at

Universitat Politècnica de València (UPV), with 10 years of field measurements [55,138] to test this. We tested the accuracy of the model by calibrating the BHE model just once and by re-calibrating the model every year.

4.1.3 Hybrid BHE Model

The analytical model represents the inside of the borehole as a single equivalent thermal resistor, i.e., it ignores the thermal capacity of the borehole. The thermal capacity of the borehole has a significant influence while predicting the performance of BHE with a time resolution in the order of an hour or smaller. Hence, the model is not suitable for hourly simulations.

ANN models can use the monitored data to represent complex relationships between the inputs and outputs. Therefore, ANN models can include the effects of natural convection in the borehole, groundwater flow, heterogeneous ground, etc., which are hard to include in analytical models. ANN models are also computationally efficient[62,64]. However, to accurately determine the output, all the variables that affect the outputs must be included in the set of inputs. Due to the large heat capacity of the ground, the performance of the BHE is affected by the entire thermal history of the ground. Therefore, selecting inputs of an ANN model that can consider the long-term performance of a BHE is challenging.

Paper II presents a hybrid analytical-ANN model to overcome the shortcomings of both the analytical and ANN model. The hybrid model uses the analytical model with a time resolution of 24-hours to include the effects of historical loads on the BHE and an ANN model with inlet temperatures and mass-flow rates of the last 24 hours to include the effects of the recent operation of the BHE.

The outputs of the analytical model, borehole wall temperatures ($BHATb_{ana}$ and $BHBTb_{ana}$), and power ($BHAP_{ana}$ and $BHBP_{ana}$) of each borehole group are included as inputs to the ANN model to combine the two models. The 24-hour thermal history of the BHE is included in the model by including measured inlet temperatures and mass flow rates as inputs. To limit the number of inputs, the 24-hour thermal history was divided into six 1-hour steps and one 18-hour step. The outputs of the analytical model are updated every 24 hours. Therefore, the current time step t can be 1 to 24 hours after the last step of the analytical model. This information is provided to the ANN model by introducing the number of hours after the last analytical step, N_{aa}, as an input to the ANN model. There is a total of 37 inputs to the ANN model, as shown in Figure 9. the power of each borehole group at time t ($BHAP_t$ and $BHBP_t$) were chosen as the outputs of the model.

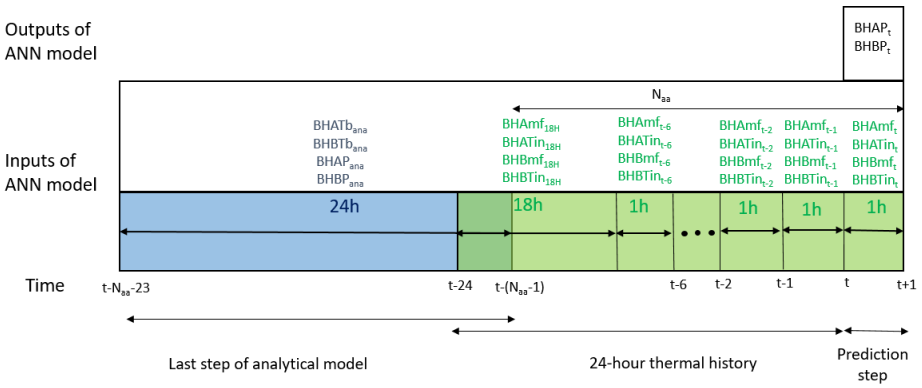

Figure 9: Inputs and outputs of the ANN model for BHE represented on a timeline (adopted from Paper II)

The initial model had 37 inputs, 2 outputs, and one hidden layer with 27 nodes. Data from January 2017 to July 2020 was used for training, validation, and testing of the model. The first two years of data were used for training, and the next one year was used for validation, and the rest was used for testing. The model was trained using the Levenberg-Marquardt (LM) algorithm.

A number of measures were used to improve the performance of the model. An ensemble of networks was used instead of a single one to improve the accuracy and reduce the overfitting of the ANN. The ensemble of networks is shown to have a lower error than the best of individual networks. The error reduces with the number of networks in the ensemble, but the improvement was negligible after a certain number of networks.

The number of hidden nodes was selected based on the validation error. The validation error decreases with an increase in the number of nodes until a certain point. Further increase in the number of hidden nodes will increase the validation error. This is because the model overfits the training data. Therefore, the model with the least validation error was chosen.

The thermal history was divided into six hours of non-aggregated steps and one 18 hour aggregated step. Increasing the number of non-aggregated steps increases the number of input nodes. Hence choosing the number of non-aggregated steps is similar to choosing the number of nodes in the input layer. Therefore, the number of non-aggregated steps was chosen using the validation error. Different optimization algorithms were also tested.

4.2 Heat pump model

The aim of this section is to develop an accurate model for a heat pump that uses the monitored data (RO3). The use of data-driven models for heat pumps is a common practice. However, most models are based on using the performance data from the manufacturer; consequently, the models are simple regression models that can be trained using a limited number of data points. The real operating condition is usually different from the ideal conditions used to generate data by the manufacturer. Hence, we can expect the models trained on data from the manufacturer to have lower accuracy when representing the real operation. Using measured data from real operations can improve the performance of heat pump models.

In Paper III, we compared the performance of five regression models and two ANN models trained using data from the manufacturer and measured data from the real operation. The accuracy of models trained using manufacturer's data was compared to the accuracy of models trained using the measured data. The comparison also shows which models are more suited when only manufacturer's data is available (in the design phase) and when measured data is available (in the operation phase). In Paper IV, we presented an ANN model to represent the three heat pumps in the GSHP system as a single unit, as described in section 4.2.2

4.2.1 Individual models

Heat pumps 1 and 2 (HP1&2) are the same type of heat pump. Therefore, both the heat pumps were represented using the same model. Heat pump 3 (HP3) operates only to produce domestic hot water, and on the coldest days, therefore it has fewer hours of measured data. However, the two circuits operate independently; hence, to increase the number of points, the two circuits were considered separate heat pumps.

Five regression models and two ANN models were tested. Table 2 shows the list of models. The regression models approximate the COP of the heat pump using polynomials with a different number of terms. The coefficients of the terms are estimated using the data. The simplest regression model considered in this thesis is the bilinear model with 4 terms, and the most complex is the multivariate polynomial model with 9 terms. Two ANN models were considered, one with two inputs and the other with three inputs. Both the ANN models had one hidden layer with five nodes and one output, COP.

Table 2: Models used for comparison (Adopted from Paper III)

Model	Equation	Inputs
Bilinear	$COP = (b_0 + bT_E) \times (b_2 + bT_E)$	T_C, T_E
Biquadratic 1	$\frac{1}{COP} = b_0 + b_1\frac{1}{Q_C} + b_2Q_C + b_3\frac{T_c}{Q_c} + b_4\frac{T_C^2}{Q_c} + b_5T_C + b_6Q_CT_C + b_7T_C^2 + b_8Q_CT_C^2$	T_C, Q_C
Biquadratic 2	$Q_C = bq_1 + bq_2T_E + bq_3T_C + bq_4T_ET_C + bq_5T_E^2 + bq_6T_C^2$ $P = bp_1 + bp_2T_E + bp_3T_C + bp_4T_ET_C + bp_5T_C^2 + bp_6T_C^2$ $COP = Q_C/P$	T_C, T_E
Multivariate Polynomial	$COP = b_0 + b_1Q_C + b_2T_E + b_3T_C + b_4Q_C^2 + b_5T_E^2 + b_6T_C^2 + b_7Q_CT_E + b_8Q_CT_E + b_9T_ET_C$	T_C, T_E, Q_C
ASHRAE	$\frac{1}{COP} = b_0 + b_1\frac{(T_C - T_E)}{Q_C} + b_2\frac{(T_C - T_E)^2}{Q_C} + b_3\frac{1}{Q_C} + b_4Q_C + b_5(T_C - T_E)$	T_C, T_E, Q_C
Neural Network 2 (NN_2)	-	T_C, T_E
Neural Network 3 (NN_3)	-	T_C, T_E, Q_C

All seven models were trained using the manufacture's data (manu_fit) and the measured data (meas_fit). The manufacturer (EnergyMachines) provided full load performance data for every combination of evaporator temperature and condenser temperature within its operating range. Measured data from April 2017 to March 2019 were used in this study. The measured data was divided into two subsets, and one was used to train the meas_fit models and the other for testing both manu_fit and meas_fit models. One year of data from April 2017 to April 2018 was used as training data for HP1 &2, and the rest was used for testing. The reason for this distribution was to cover the full range of operation of HP1&2 in the training data and evaluate the ability of the model to predict future performance. The measured data for HP3 was scattered over time, so 50% of the measured data was randomly selected as training data.

The two ANN models used were simple models with two or three inputs. Simple models were chosen so that they can be compared with other regression models. However, ANNs are flexible models that can easily be improved to better utilize the measured data. The input, outputs, and architecture of the ANN can be modified according to the available data. A systematic method to improve the ANN model was presented in Paper IV. Three measures to improve the accuracy of the ANN models were tested, including additional explanatory variables in the

model, changing the output variable, and increasing the number of nodes in the hidden layer.

Five additional explanatory variables were considered to include the effect of the partial operation, the effect of the sub-cooler, and the COP from the manufacturer's data into the model. The fraction of time the compressors are switched on (UT_r), and the ratio of actual condenser power to design condenser power (Q_{cr}) was used to consider the partial operation. The operation of the sub-cooler was represented by sub-cooler power (Q_{SC}) and sub-cooler temperature (T_{SC}). The inputs were added to the NN_3 model using greedy forward selection. At each iteration, the best input among the variables considered was added to the ANN model. The process is stopped when the improvement in the accuracy of the ANN model in an iteration is below a threshold.

COP was used as the output of the NN_3 model to compare it with other regression models. However, using compressor power as the output also conveys the same information since COP can be calculated from compressor power and Q_c. Therefore we tested if changing the output from COP to compressor power affected the accuracy of the ANN model. Increasing the number of hidden nodes will increase the variability of the ANN model. Hence it can represent more complex relationships between inputs and outputs. Therefore, the number of nodes was increased until the ANN model was observed to overfit the training data.

4.2.2 Combined model

Paper III shows that ANN models can accurately represent heat pumps when field measurements are available. Paper III also shows that ANN models are flexible and can represent complex heat pumps if the right inputs are chosen. Therefore, a single ANN model represented all three heat pumps in Paper IV. This reduced the complexity of the overall system as the distribution of load among the heat pumps was not explicitly specified. The total compressor power (CompPower) and the mass flow rate of the cooling circuit of the heat pumps (HPCoolmf), which is determined by the number of compressors on, were chosen as outputs of the ANN model.

The power of the heat pumps is determined by the heating load and cooling load in heating mode and cooling mode, respectively. Therefore, ANN models with different inputs were used for heating and cooling mode. The inputs of the heating mode model are heat produced by the heat pump (HPHeatPower), HPHeatTout, DHWPower, DWHTout, HPCoolTin, and mode number, which is number to represent the mode of the GSHP. The cooling mode model uses HPCoolPower instead of HPHeatPower as input.

The data from May 2017 to April 2021 was used to develop the model. 70% of the data was used to training the models, 15% was used for validation, and the rest was used for testing. The procedure for choosing the architecture of the ANN model was similar to the ANN models for individual heat pumps, i.e., the number of nodes was increased until the model was observed to overfit the training data.

4.3 GSHP system model

The hybrid BHE model and the combined heat pump model were used to develop a model for the entire GSHP system (RO1). The heating and cooling loads and the temperature requirements were the inputs to the model. The operation of the GSHP system was simulated, assuming a balance of power in the heating and cooling circuits at each 1-hour time step. The configuration of the heating and cooling circuit depends on the mode of the GSHP system. Therefore, at each time step, the mode of the GSHP system was determined, and the mass and power balance equations corresponding to the mode were used. The operating cost of the GSHP was calculated using the compressor power (CompPower), and the long-term stability of the ground was determined using the power of the BHE (BHP). Therefore, CompPower and BHP were the most important outputs of the model.

The GSHP system model also needed a model for the heat exchanger in the cooling circuit, i.e., HXC. An empirical model based on the log mean temperature difference (LMTD) approach was used for HXC. The coefficients of the model were determined by fitting the empirical relation to the field measurements.

In both the heating modes, the BHE is connected to the cooling circuit. In the free cooling with active cooling mode, borehole group A is connected to the heating circuit while borehole group B is connected to the cooling circuit. In the active cooling mode, both the borehole groups are connected to the heating circuit. Hence three different algorithms were used to calculate the GSHP model for the three different configurations of the GSHP. The algorithms are shown in Figure 10. All three algorithms use an initial guess for HPCoolTin and run the component models of the GSHP to calculate the residual of the power balance equation for the cooling circuit. The HPCoolTin value is then adjusted based on the residual value. This process is repeated until the residual power balance is below a threshold. The algorithm for free cooling with active cooling mode has an additional initial guess value of HPCoolPower. Hence, an additional criterion that the outlet temperature from the cooling side of the heat pump (CoolTin) matches the required cooling temperature calculated using the heat exchanger model is added.

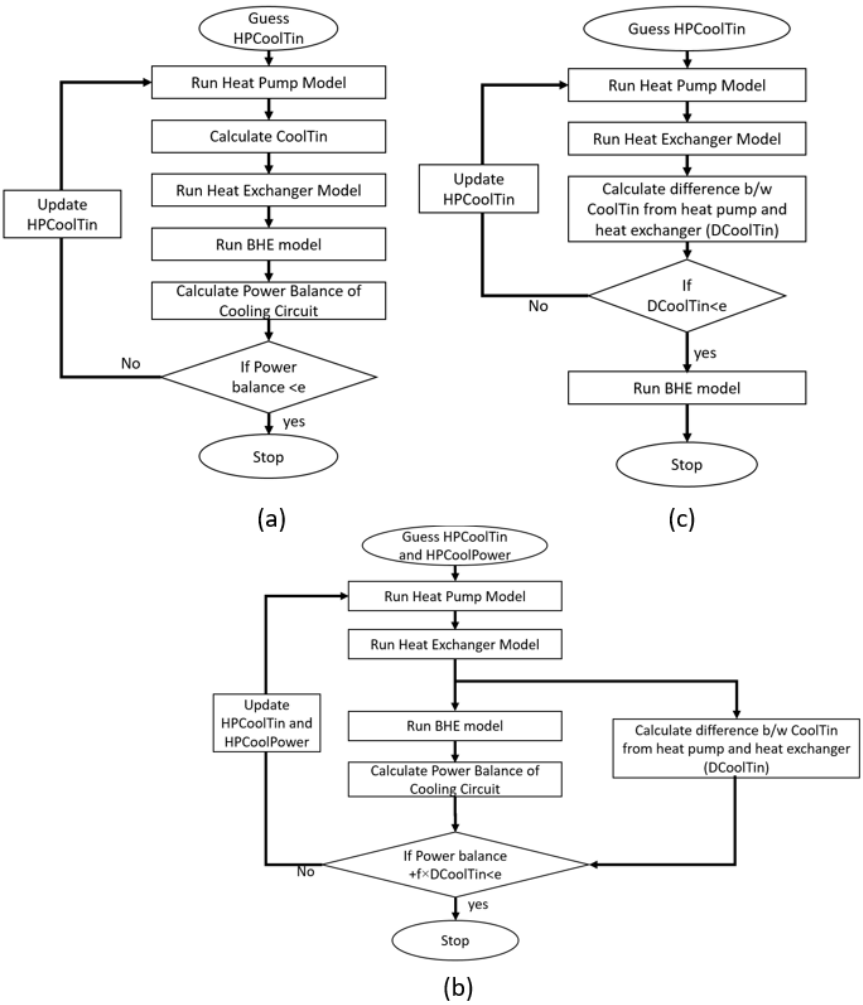

Figure 10: Flowchart for GSHP model in (a) heat modes (b) free cooling with active cooling mode and (c) active cooling mode (Adopted from Paper IV)

The mode of the GSHP system at each time step was determined based on the operation at the previous time step. The mode was changed if certain criteria were satisfied. The criteria for changing of mode was similar to the criteria in real operation, as described in Paper IV, except for active cooling mode. The temperature of the BHE was observed to increase over the years. Hence the operator of the GSHP manually changed the mode to active cooling mode for a few days in summers after 2019. Therefore, the active cooling mode was used in the simulation when the GSHP was observed to be operating in active cooling mode in real operation.

5 Operation Optimization

This chapter describes the method to achieve RO4, i.e., optimize the operation of a customer's GSHP operating in parallel to a DHC network. The optimal operation scheme was determined using one year of operation of the GSHP system. The loads and temperature requirements of the GSHP were calculated as the average of the four years of measured data. The optimization aimed to find a sustainable operation scheme with a minimal yearly operating cost of heating and cooling the building. For the operation to be sustainable in the long term, the ground temperature must be relatively stable, which was defined as a change of less than 1^{o}c in 50 years. The cost of heating the building was considered from the perspective of the energy company (Umeå Energi AB). The cost of district heating, district cooling, and electricity for the GSHP were included.

The marginal variable production cost was used for the optimization, i.e., the cost of producing the extra energy for heating and cooling of the area. The cost of producing district heating and cooling using the least preferred production unit operating at a particular time was considered as the marginal cost of district heating and cooling, respectively. The production cost and information about the production units operating at each hour were provided by the energy company. The cost of fuel, taxes and transmission losses were considered in the cost calculation. Since marginal electricity comes from the regional grid, i.e., it is not produced by the energy company. Hence, the cost of buying electricity from the regional grid was considered as the marginal cost of electricity. Taxes and transmission costs were added to the production cost.

One year of operation with the existing scenario was first simulated to establish a baseline for comparison with other scenarios. The inputs for the simulation, i.e., loads and temperature requirements, were calculated as the average of the four years of measured data. CompPower from the model was used to calculate the hourly electricity load. The district heating and cooling loads were also calculated as the average of the four years. The loads, along with the hourly cost of electricity, district heating, and district cooling, were used to calculate the total cost of energy production. The monthly average power of the BHE for one year was calculated using the simulated BHP. To estimate the long-term effect of imbalance in the load, the monthly average load was repeated 50 times. The change in temperature of the ground over 50 years was estimated using the analytical model.

An operation scenario to minimize the cost was simulated. To minimize the cost, the least expensive source of heating or cooling was used at each time step. The GSHP cannot replace a part of the district heating load due to the higher temperature requirement of some of the buildings in the area. Hence only the

part of district heating that can be replaced by the GSHP was considered in this analysis. The GSHP system uses electricity to provide both heating and cooling, but the power of the heat pump is decided by the dominant load. Reducing the power of the heat pump up to a certain point will only reduce either heating or cooling provided by the GSHP system. Therefore, the cost of providing the dominant load was compared with district heating or cooling. If the heating/cooling from the GSHP system was cheaper, the GSHP was operated at maximum capacity or to satisfy both heating and cooling demands (max mode). Otherwise, the GSHP was operated at a power at which both heating and cooling from the GSHP are utilized (base mode).

In the optimal scenario, the cost must be minimized while maintaining a stable temperature in the ground. To make the operation of the BHE balanced, the threshold for switching between max and base modes was modified. An additional cost ϵ was introduced to the GSHP system cost. The criteria for the GSHP system to operate in max mode was changed to:

Heating mode,

$$\frac{Marginal\ cost\ of\ elecrticity}{COP_{Heat}} + \epsilon < Marginal\ cost\ of\ district\ heating \quad (3)$$

Cooling mode,

$$\frac{Marginal\ cost\ of\ elecrticity}{COP_{Cool}} - \epsilon < Marginal\ cost\ of\ district\ cooling \quad (4)$$

6 Summary of Results

This chapter presents the main results of the thesis obtained using the methods described in chapters 4 and 5. The performance of the models developed to achieve RO1, RO2 and RO3 are presented in section 6.1, and the results of optimization of operation of the GSHP are presented in section 6.2.

6.1 Models of GSHP using monitored data

Section 6.1.1 presents the results of the two approaches used to improve BHE models using the field measurements. Section 6.1.2 presents results of heat pump models that use field measurements

6.1.1 BHE Model

6.1.1.1 Calibration of the model

The performance of the BHE was simulated for the period from February 2016 to February 2019 with a time resolution of one day. The root mean square (RMS) deviation between the measured and simulated load of the uncalibrated model was 85 kW, which is 22.3% of the absolute average load. The simplification of the physical phenomenon by the model, uncertainty in the model parameters, and uncertainty in the measured data are some of the reasons for the deviation.

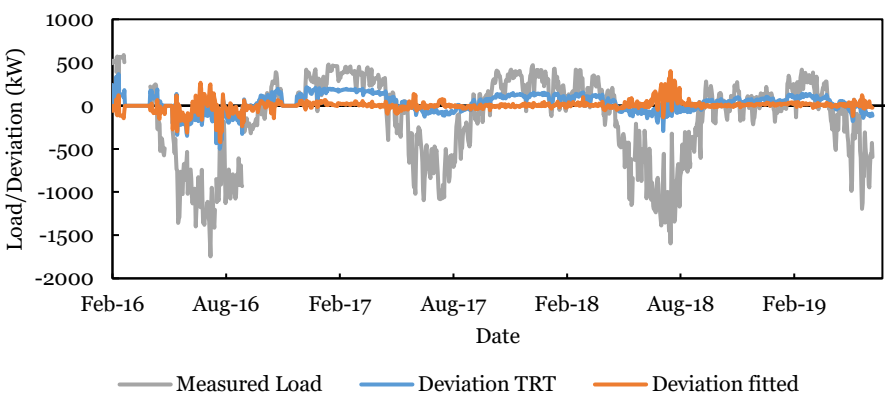

Figure 11: Measured load, deviation of the uncalibrated model, and deviation of the calibrated model (adopted from Paper I)

Figure 11 shows the measured load along with the deviation of the uncalibrated (Deviation TRT) and the calibrated model (Deviation fitted). Calibration reduced the RMS deviation from 85 kW to 52kW. However, it was observed that the

estimated properties were outside the uncertainty range of the measured values. This shows that the calibrated values are compensating for imperfections in the model. The calibrated model parameters must not be considered as accurate values of the thermal properties of the ground.

The model parameters were calibrated using three different time resolutions for the model, 30 days, 1 day, and 6 hours. The calibrated parameters were used to simulate the performance of the BHE with a time resolution of 30 days, 1-day, 6-hours, and 1-hour. The results showed that parameters from 1 day and 6-hour time resolution were similar, with similar RMS deviation for all four time resolutions. The parameters from the 30-day time resolution were different from the other two, and the RMS deviation of the model using the model parameters was higher. This indicates that the 30-day time step is too large to accurately differentiate the effects of each parameter. However, a time resolution of 1 day can be sufficient to differentiate the effects of each parameter using the analytical model. Hence using a time resolution of 1 day for calibration was recommended.

The calibration data was divided into four 4-month long periods and two seasons for extraction and injection to test if using a different set of parameters for different seasons improves the performance of the BHE model. Two different scenarios were tested, using four sets of parameters for four seasons and using two different sets of parameters for extraction and injection. The RMS deviation was 51 kW and 50 kW while using four and two sets of parameters, respectively. Therefore, using different sets of parameters for injection and extraction reduced the deviation. In the initial analytical model, different R_b values were used for injection and extraction, but the value for R_b for extraction was obtained by adding a constant value to the R_b value for injection, which is a common practice in Sweden. However, the results indicate that this method is not sufficient to account for the difference in ground properties for injection and extraction.

A BHE with 10 years of monitored data was used to check if recalibrating the model parameters every year improves the performance of the BHE model. The uncalibrated model had an RMS deviation of 27%. Calibrating the model once after 4 years of operation reduced the error to 23 % while recalibrating the model every year after the 4th year reduced the error to 21%, indicating that recalibrating the model every year improves the model accuracy.

6.1.1.2 Hybrid model

The relative RMSE of the initial hybrid model was 3.2%, 6.1%, and 7.3% for training, validation, and testing, respectively. The overall model had a relative RMSE of 4.9%, which is significantly lesser than the analytical model or the calibrated analytical model. Table 3 shows the result of various measures to improve the hybrid model.

Table 3: Result of improvement measures to the hybrid model

Improvement measures	Value selected	Relative RMSE (%)		
		Training	Validation	Testing
Initial model		3.20	6.1	7.3
Ensemble	15 ANNs	2.7	5.9	6.7
No of hidden nodes	45 nodes	2.4	5.6	6.3
Optimization algorithm	LM	2.4	5.6	6.3
No of non-aggregated steps	6 steps	2.4	5.6	6.3

The performance of the final model was compared with the performance of the analytical model, the calibrated analytical model, and three different types of neural network models.

The moving average of the analytical model calibrated analytical model and the hybrid model is shown in Figure 12. The hybrid model clearly performs better than the other two models. The RMSE of the hybrid model for 2020 is 6.3% compared to 21.9% for the analytical model and 13.9% for the calibrated analytical model. The computational time of the hybrid model was also significantly lower than the analytical model, 15 minutes compared to 5 hours.

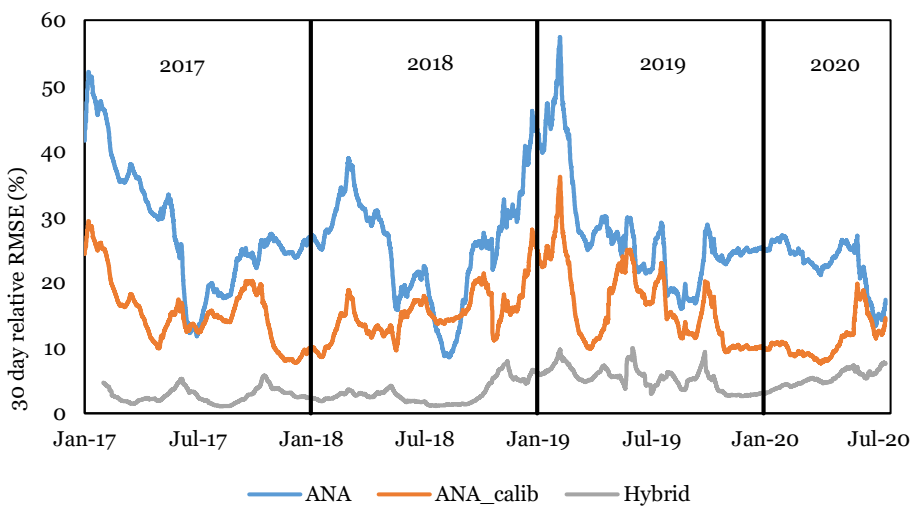

Figure 12: 30-day moving average of relative RMSE of the analytical model, calibrated analytical model, and the hybrid model (adopted from Paper II)

The hybrid model was also compared to a regular ANN model, a recursive neural network (RNN) model, and a gated recursion unit (GRU) model. Figure 13 shows the comparison of the moving RMSE of the models. The hybrid model has the lowest RMSE among the models. The RMSE for the testing period is 6.3%, 13.4%, 12.5%, and 13% for the hybrid model, the ANN model, the RNN model, and the GRU model, respectively. Hence, the hybrid model performs better than both analytical and ANN models in this study.

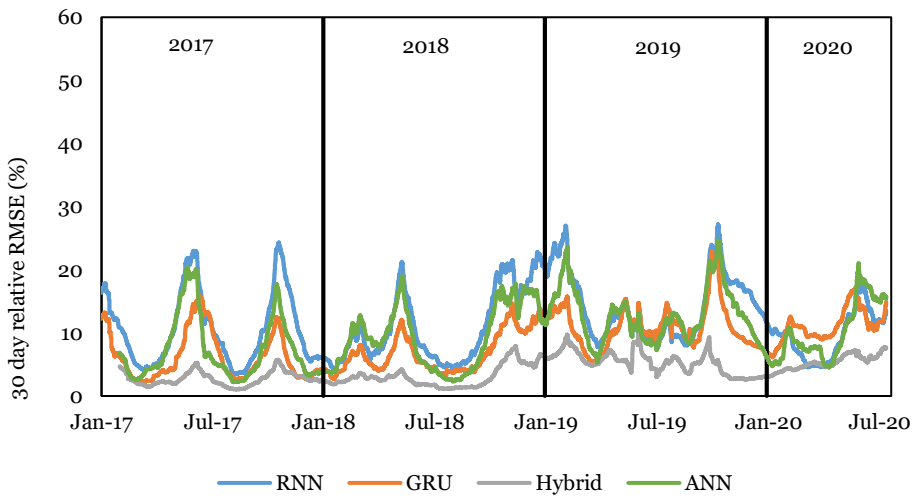

Figure 13: 30-day moving average of relative RMSE of the RNN model, GRU model, ANN model, and hybrid model (adopted from Paper II)

The hybrid model was used in the model of the GSHP system since it is clearly better than the other models tested. Two minor changes were made to the hybrid model to make it more suitable for the GSHP system model. Firstly, since the model was already validated and more measured data were available, 80% of the data from May 2017 to April 2021 was used for training, and the other 20% was used for validation. Secondly, the best model was used instead of an ensemble of 15 models to decrease the computational time to the model. The relative MAE of the updated model was 4.24% compared to 3.54% of the model from Paper II.

6.1.2 Heat pump model

6.1.2.1 Comparison of models

All 7 models were trained on the data from the manufacturer and the data from actual operation. As expected, the manu_fit models had a lower training error than mes_fit models. The error for HP3 is higher than HP1&2 since HP3 has a

larger operating range than HP1&2. Among the manu_fit models, the NN_3 model has the least training error, 0.2% for HP1&2 and 0.6% for HP3, and the biquadratic 1 model has the least training error among the regression models, 0.5% for HP1&2 and 3.0% for HP3. The NN_3 model also has the lowest training error among mes_fit models, 5.2% HP1&2 and 7.1% for HP3. The range of training RMSE among the models is much higher for manu_fit (0.2%-20.6%) compared to meas_fit (5.2%-8.9%); this implies that the choice of model is not important for meas_fit, indicating that the error in meas_fit models is not due to the choice of function to represent the relationship between the inputs and outputs but due to variables not considered in the models.

The testing error of the models is shown in Figure 14. The error of the meas_fit models is lower than the manu_fit models since the training and testing data for the meas_fit model are similar. Among the manu_fit models, the bilinear model, which is the simplest model, has the least error while more complex models like the NN_3 model and multivariate polynomial models perform poorly. This indicates that in the design phase when limited data is available, it is better to use simple models since more complicated models are more likely to overfit the data, which may not be representative of the real operation. The NN_3 model has the least testing relative RMSE among the meas_fit models, 6.4% for HP1&2 and 7.5% for HP3. Indicating that when measured data from the actual operation is available, more complex models, like ANN models, are better at utilizing the data to deduce accurate relationships between inputs and outputs

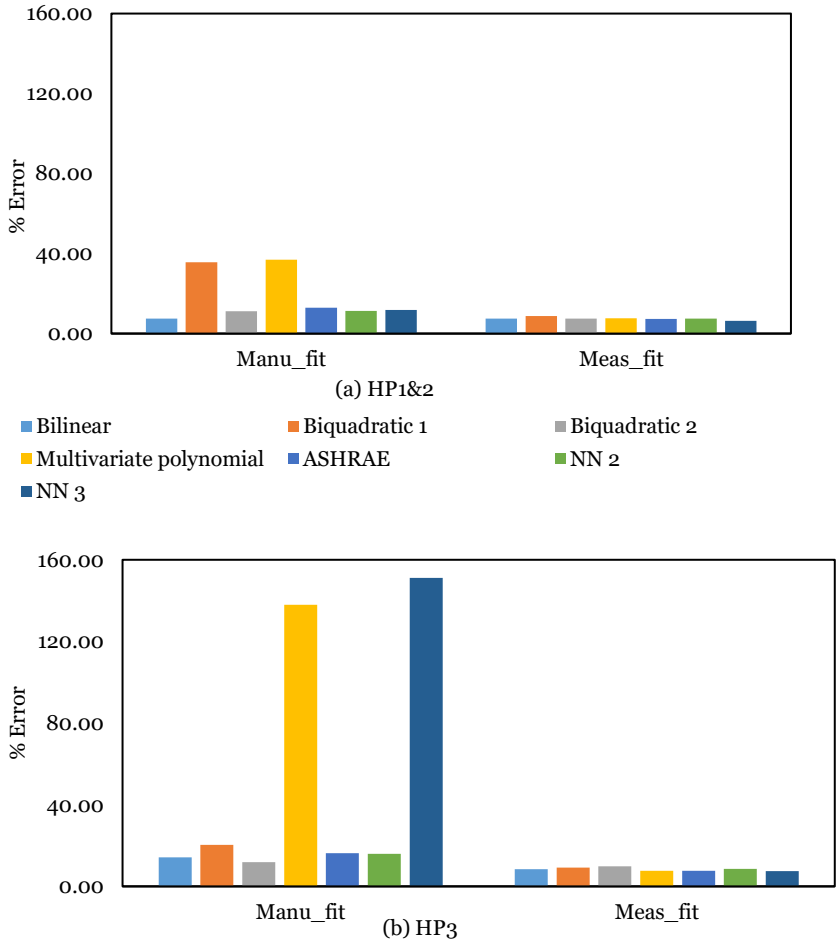

Figure 14: Relative testing errors of the models for (a) HP1&2 and (b)HP3 (adopted from Paper III)

6.1.2.2 Improvement of ANN model

The ANN model was first improved by adding more inputs to the NN_3 model. Five inputs were tested, UT_r, Q_{cr}, Q_{SC}, $T_{SC,}$ and COP_{manu}. The best inputs were sequentially added to the model until the improvement in the model was below a threshold. Two different thresholds were used, 1% and 0.1%. Two models for HP1&2 and HP3 were selected based on the two thresholds. ANN models with four inputs, T_E, T_C, $Q_{C,}$ and Q_{SC} (NN_4Q_{SC}), and five inputs, T_E, T_C, Q_C, $Q_{SC,}$ and T_{SC} ($NN\_5Q_{SC}T_{SC}$), were selected for HP1&2 and the NN_3 model and NN_4Q_{SC} were selected for HP3. The NN_4Q_{SC} and $NN\_5Q_{SC}T_{SC}$ models for HP1&2 had testing relative RMSE of 4.9% and 4.6%, respectively. The testing relative RMSE of models for HP3, NN_3, and NN_4Q_{SC} were 7.5% and 7%, respectively.

The outputs of the four selected models were changed from COP to compressor power. Changing the output did not improve the models for HP1&2, but the models for HP3 improved significantly. The training error of the NN_3 with compressor power as output (NN_3PO) was reduced to 4.8%, and the training error for NN_4Q_{SC}PO was 4.6%. Hence, NN_3PO and NN_4Q_{SC}PO were selected for further improvements.

In the next step to improve the model, the number of nodes in the hidden layer was varied for the four selected models, and the architecture with the least training error was selected. An architecture with 15 hidden nodes was selected for NN_4 $Q_{SC,}$ and architectures with 10 hidden nodes were selected for the other three models. The testing error of NN_4Q_{SC}, NN_5$Q_{SC}T_{SC}$, NN_3PO and NN_4Q_{SC}PO were 4.6%, 4.5%, 4.4% and 4.3% respectively. The testing error of all four models were less than 5%

The results of this section demonstrate that ANN models can accurately represent the behavior of heat pumps. The results also highlight the importance of the choice of inputs and output for an ANN model.

6.1.2.3 Combined model

The number of nodes was chosen based on the normalized validation error of both the outputs, i.e., CompPower and HPCoolmf. An architecture with two hidden layers with 35 nodes in each layer was chosen for the heating mode model, and two hidden layers with 30 nodes in each layer were chosen for the cooling mode model.

The relative MAE of the heating mode model was 3.7% for CompPower and 3.1% for HPCoolmf, and for the cooling model, the relative MAE were 4.29% and 3.2% for CompPower and HPCoolmf, respectively. The results of the two models were combined by using the heating mode model during the heating season and the cooling mode model during the cooling season. The relative MAE of the complete model was 3.77% and 3.31% for CompPower and HPCoolmf, respectively.

6.1.3 GSHP model

The model of the GSHP system was validated using 4 years of measured data from May 2017 to April 2021. The main outputs of the model were CompPower and BHP. The simulation time for 4 years of the hourly simulation was around 9 hours on a standard computer. Figure 15 shows the moving average of measured and simulated CompPower along with the deviation between the two. The relative MAE for CompPower was 7.3%.

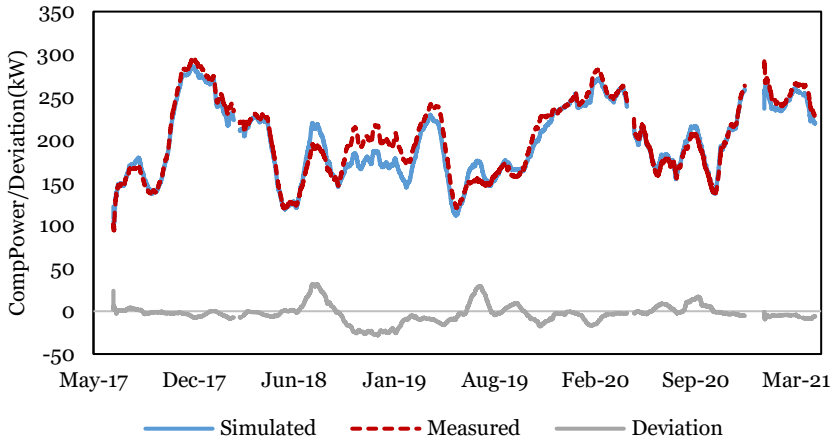

Figure 15: 30-day moving average of measured power, simulated power, and deviation of CompPower (adopted from Paper IV)

Figure 16 shows the moving average of measured and simulated BHP and the deviation between the measured and simulated values. The relative MAE of BHP is 19.1%, and the average measured heat extracted from the ground was 47 kW higher than the simulated value. The MAE is around 4.5 times higher than the MAE of the individual model for BHE. This indicates that the error in BHP is not due to the BHE model but due to an error in other components of the GSHP system. Three possible reasons for the error were explained in Paper IV. Firstly, the model for HXC had low accuracy, with an RMSE of 17.6% in determining the value of U×A. Secondly, since the actual modes of operation of the GSHP system were not recorded, determining accurate criteria to classify the modes was a challenge. Thirdly, since a steady-state model was used for the simulation, it was assumed that the GSHP system followed the control objectives. However, examples of the control objective not being followed were observed from the measured values.

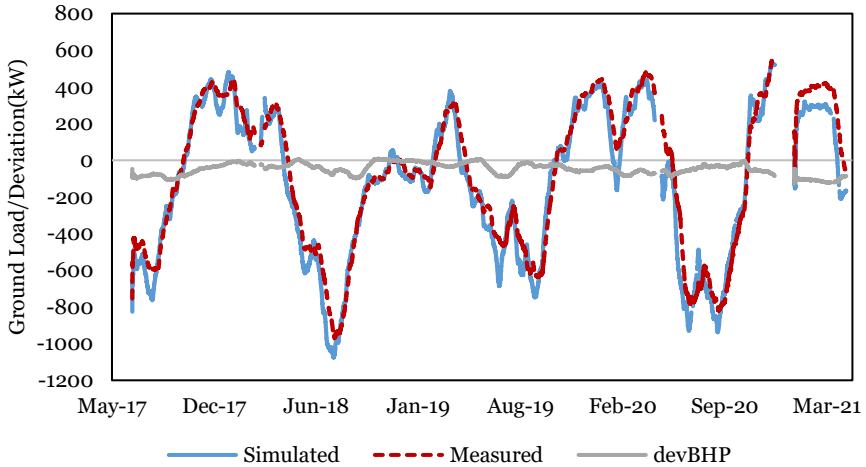

Figure 16: 30-day moving average of measured power, simulated power, and deviation of BHE power (adopted from Paper IV)

The results indicate that the GSHP system model is a good representation of the real system, even though there is room for improvement in the GSHP model.

6.2 Operation Optimization

The present operational scenario was simulated for 1 year using the average of 4 years of measured data as inputs to the model. The district heating and cooling loads were also calculated as the average of the 4 years. In the present scenario, 54.4% of the heating load and 91.6 % of the cooling load were provided by the GSHP system, while the rest is provided by the district heating and cooling network. Note that only the part of the heating load that can be replaced by the GSHP was considered in this study. The annual marginal cost of the energy company for providing heating and cooling for the buildings was 322 t€. The marginal CO_2 was 1220 tons. A 50-year simulation of the ground using the BHP load from the simulation showed that the temperature of the ground would increase by 12°C if the operation scheme were not changed.

In the minimal cost scenario, the cheaper of the two alternatives, GSHP or district heating/cooling, is used at each time step without considering the long-term stability of the ground. The operational cost of heating and cooling the buildings was reduced by 69 t€, and the CO_2 emissions were reduced by 175 tons in this scenario. However, this operational scenario is not sustainable since the average borehole wall temperature was shown to reduce by 24°C in 50 years for this scenario.

In the optimal scenario, the criteria for choosing between base and max mode for the GSHP system was changed to equations 3 and 4. Since there was a reduction in temperature in the minimal cost scenario, the heat extracted from the BHE in the heating mode must be decreased, and the heat injected into the BHE in cooling mode must be increased. Therefore, ϵ must have a positive value. The value ϵ was varied using trial and error until the change in average borehole wall temperature (ΔT_b) after 50 years of operation was less than 1°C. Figure 17 shows the variation of ΔT_b after 50 years and the annual savings in operation cost with a change in ϵ. The black lines mark the acceptable range of ΔT_b after 50 years.

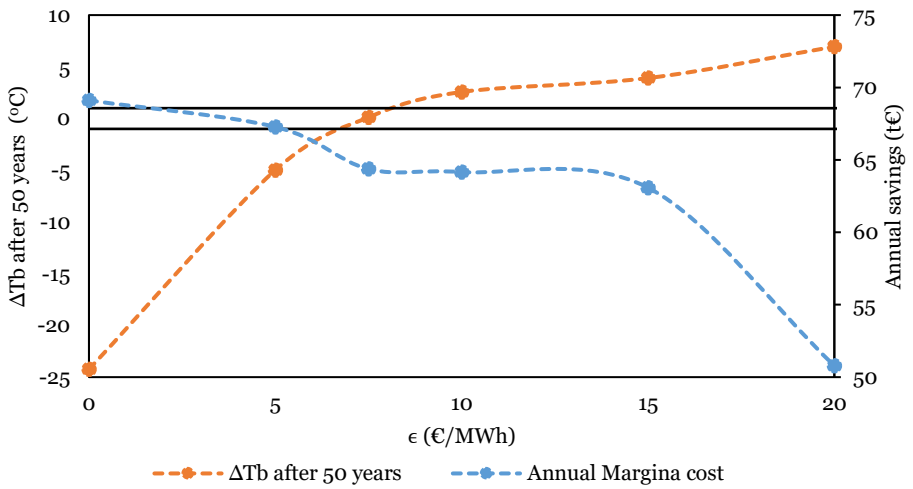

Figure 17: Variation of change in Tb after 50 years of operation and annual savings with ϵ along with acceptable limits for ΔTb after 50 years (adopted from Paper IV)

The ϵ value of 7.5 €/MWh was chosen for the optimal case. The annual cost of operation was reduced by 64 t€, and the annual CO_2 was reduced by 92 tons in the optimal case, while the ΔT_b after 50 years was less than 1°C. Figure 18 shows the moving average of the percentage of heating and cooling loads satisfied by the GSHP system. 69.6% of the heating load and 96.8% of the cooling load of the buildings were covered by the GSHP system in the optimal scenario.

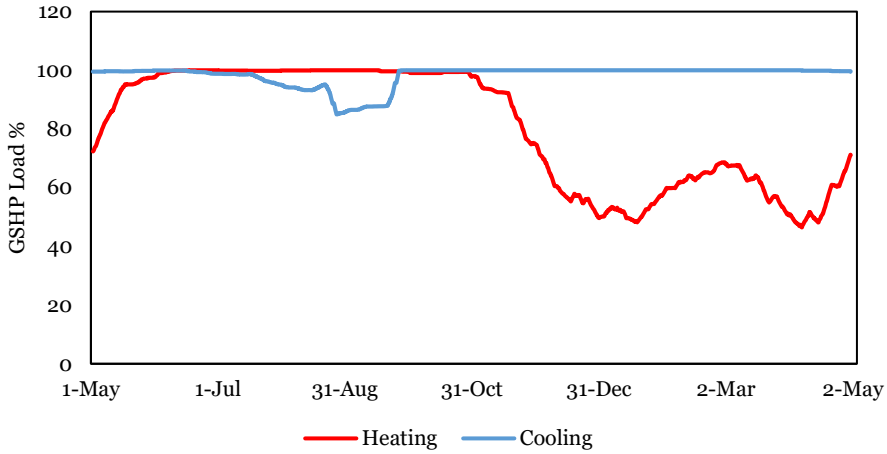

Figure 18: Moving average of the percentage of heating and cooling loads covered by the GSHP (adopted from Paper IV)

7 Discussion

GSHPs can be used to store both heat and cold for long periods. Additionally, due to their connection to the electrical network, they also provide the option of storing excess energy in the electrical network from renewable sources like solar and wind in the form of heat or cold. Hence, GSHP can provide flexibility to the energy system. This thesis demonstrates the benefits of proper utilization of the flexibility provided by GSHPs. The results show that improvement in the operation of GSHP is economically beneficial and can extend the lifetime of the GSHP. Therefore justifying the need for accurate models for GSHPs in operation.

The models developed in this thesis use field measurements to represent the GSHP accurately. The results show that the hybrid model for BHE and the ANN model for the heat pumps are accurate. Hence, these models are important contributions of the thesis. The models can be adopted in various applications including fault detection and optimization of other GSHPs.

The performance of the models presented in this thesis is influenced by the quantity and quality of data available. Therefore, to gain a better understanding of the capabilities of the models they need to be tested on different sets of field measurements. A limitation of data-driven models is the deterioration of performance when the inputs are out of bounds of the training data. Hence, the models can be applied to a wider variety of problems by studying the deterioration of models while extrapolating and identifying methods to reduce the deterioration.

In this thesis, the GSHP model is used to optimize the load distribution between the GSHP and the DHC network. The optimization method minimizes the cost at each time step while introducing a penalty to ensure the long-term stability of the ground. This simple method of considering the long-term stability of the ground in optimization is a contribution of this thesis that can be applied to optimize the operation of any hybrid GSHP. However, this method has some limitations that can be addressed in future studies. For example, the heating and cooling demand and the cost of production were calculated based on historical data. The change in demand and production in the coming years can be considered in future studies. In the present method, the best heating and cooling option for the current time step is determined based on the current cost and the long-term stability of the ground. This approach simplifies the optimization problem to a single variable problem. However, a lower operation cost can be achieved if the load distribution of all the time steps is determined simultaneously or by using a moving time horizon. Future studies can explore such optimization methods. Adjusting the load distribution between the GSHP and the DHC network is not

the only way to optimize the operation of the heating and cooling system. Future studies can also explore other options to improve the operation, like changing the control strategy or set points of the GSHP, connecting more buildings to the GSHP system, adding more heating/cooling capacity to the GSHP, etc.

The cost of heating and cooling the hospital buildings was optimized from the perspective of the energy company, but the GSHP system belongs to the hospital. Hence to minimize the cost of production, the energy company must cooperate with the hospital. The results presented in this thesis can help to convert the hospital from a consumer to prosumer. However, the task of determining the exact terms of cooperation for such prosumers is challenging and should be addressed in further studies.

9 Conclusion

This thesis demonstrates that operating a customer's GSHP system in a district heating and cooling network in cooperation with the energy company benefits both the building owner and the energy company. We developed models for GSHP and its components that utilize the field measurements to accurately represent the GSHP system. The models were used to achieve the objective of minimizing the cost of producing energy for heating and cooling of the area while ensuring a sustainable operation of the GSHP system.

Two approaches to improve the accuracy of an analytical model of BHE were presented. In the first approach, the thermal parameters of the analytical model were calibrated. Calibration of the parameters reduced the relative RMSE from 22% to 14%. The second approach used a hybrid analytical-ANN model. The hybrid model had a relative RMSE of 6.3% for the testing period and computationally it was 20 times faster than the analytical model. Therefore, the hybrid model was chosen to represent the BHE.

The performance of seven data-driven models for heat pumps were compared to show that ANN models are suitable when measured data from the actual operation is available. Hence ANN models were used to represent the heat pumps in the model of the GSHP system. A single ANN model was used to represent all three heat pumps of the GSHP system, which simplified the model. The ANN model for the heat pumps had a relative RMSE of 3.8% when simulating compressor power.

The hybrid BHE model and the ANN model for heat pumps were used in the GSHP system model. The model was validated using 4 years of measured data. The MAE for compressor power and the power of the BHE was 7.3% and 19.1%, respectively.

A method to determine the optimal load distribution between the GSHP system and the DHC network using the GSHP system model was presented. In optimal operation, the annual cost of operation for the energy company could be reduced by 64 t€ compared to the existing scenario and the ground temperature could be stable. The CO_2 emissions could be reduced by 92 tons per year in the optimal scenario.

This thesis shows that the cost and CO_2 production of the energy company can be reduced through a customer's GSHP. Therefore the energy company could consider a GSHP system as an asset in the DHC network and cooperate with the building owner to benefit from it. The building owners can also benefit from the

cooperation by ensuring the sustainability of the GSHP and by developing a prosumer relationship with the energy company. This thesis has contributed to the field of GSHPs and DHC by developing methods to determine the optimal operation of such systems and by developing models that are required for optimization.

Acknowledgments

This thesis is a result of a supportive environment and a great deal of assistance received during my Ph.D. I would like to thank everyone, directly and indirectly, involved in the project.

Firstly, I thank my supervisors' Thomas Olofsson, Staffan Andersson, and Ronny Östin for their constant encouragement and brilliant guidance. It would be impossible to navigate through the Ph.D. without their advice and support.

I am grateful to Umeå Energi AB., Jörgen Carlsson in particular, for providing insights into the working of a DHC network and for providing the data on the production of DHC. I also express my gratitude to Region Västerbotten and Instituto Universitario de Investigación de Ingeniería Energética at Universitat Politècnica de València for providing measured data from their respective GSHP systems. I thank Kristofer Linder and Jesper Burlin for taking the time to explain the working of the GSHP system at the University Hospital in Umeå. I am grateful to EnergyMachines for providing information about GSHP installation at Umeå.

I would like to thank Zonghua Gu for his insights and suggestions in the development of the neural network models

I thank everybody at the Department of Applied Physics and Electronics for providing an engaging and fun work environment. I thank Helena, Ismael, Ramtin, Antonio, Naresh, Ola, Mark, Jimmy, Hongxia, and especially Shoaib for their companionship and Fika room discussions. I am grateful to the administrative staff, Christer Rönnqvist, Robert Sjöblom, Leif Johansson, Helena Glenge, Maria Rönnberg, and Martina Sundling for their vital support.

I thank my colleagues at Industrial Doctoral School, especially Ivan Riumkin, for providing feedback on my research from different perspectives. I would like to acknowledge the incredible effort from Benkt Wiklund and other staff members at Industrial Doctoral School in the planning and organization of various events at Industrial Doctoral School.

I am forever indebted to my parents and my sister for their love and support. I thank my mother for keeping my spirits high throughout my Ph.D. I thank Usha aunty for her feedback on my thesis. I thank Akshara for listening to me ramble on about my work.

Industrial Doctoral School at Umeå University and Umeå Energi AB. are gratefully acknowledged for their financial support.

References

1. Fleiter, T.; Steinbach, J.; Ragwitz, M.; Dengler, J.; Köhler, B.; Reitze, F.; Tuille, F.; Hartner, M.; Kranzl, L.; Forthuber, S. Mapping and analyses of the current and future (2020-2030) heating/cooling fuel deployment (fossil/renewables). *Eur. Comm. Dir. Energy* **2016**.

2. Eurostat: Renewable Energy for Heating and Cooling Available online: https://ec.europa.eu/eurostat/web/products-eurostat-news/-/ddn-20200211-1 (accessed on Aug 2, 2021).

3. European Commission *An EU Strategy on Heating and Cooling, COM(2016) 51 Final*; Brussels, Belgium, 2016;

4. Connolly, D.; Lund, H.; Mathiesen, B.V.; Werner, S.; Möller, B.; Persson, U.; Boermans, T.; Trier, D.; Østergaard, P.A.; Nielsen, S. Heat Roadmap Europe: Combining district heating with heat savings to decarbonise the EU energy system. *Energy Policy* **2014**, *65*, 475–489.

5. David, A.; Mathiesen, B.V.; Averfalk, H.; Werner, S.; Lund, H. Heat roadmap Europe: large-scale electric heat pumps in district heating systems. *Energies* **2017**, *10*, 578.

6. Lund, H.; Werner, S.; Wiltshire, R.; Svendsen, S.; Thorsen, J.E.; Hvelplund, F.; Mathiesen, B.V. 4th Generation District Heating (4GDH): Integrating smart thermal grids into future sustainable energy systems. *Energy* **2014**, *68*, 1–11.

7. Werner, S. District heating and cooling in Sweden. *Energy* **2017**, *126*, 419–429.

8. Gehlin, S.; Andersson, O.; Rosberg, J.-E. Country Update for Sweden 2020. In Proceedings of the Proceedings, World Geothermal Congress 2020; 2020.

9. Åberg, M.; Fälting, L.; Lingfors, D.; Nilsson, A.M.; Forssell, A. Do ground source heat pumps challenge the dominant position of district heating in the Swedish heating market? *J. Clean. Prod.* **2020**, *254*, 120070.

10. Le Truong, N.; Gustavsson, L. Costs and primary energy use of heating new residential areas with district heat or electric heat pumps. *Energy Procedia* **2019**, *158*, 2031–2038.

11. Kontu, K.; Vimpari, J.; Penttinen, P.; Junnila, S. Individual ground source heat pumps: Can district heating compete with real estate owners' return expectations? *Sustain. Cities Soc.* **2020**, *53*, 101982.

12. Averfalk, H.; Ingvarsson, P.; Persson, U.; Gong, M.; Werner, S. Large heat pumps in Swedish district heating systems. *Renew. Sustain. Energy Rev.* **2017**, *79*, 1275–1284.

13. Carvalho, A.D.; Moura, P.; Vaz, G.C.; de Almeida, A.T. Ground source heat pumps as high efficient solutions for building space conditioning and for integration in smart grids. *Energy Convers. Manag.* **2015**, *103*, 991–1007.

14. Li, M.; Li, P.; Chan, V.; Lai, A.C.K. Full-scale temperature response function (G-function) for heat transfer by borehole ground heat exchangers (GHEs) from sub-hour to decades. *Appl. Energy* **2014**, *136*, 197–205, doi:https://doi.org/10.1016/j.apenergy.2014.09.013.

15. Zeng, H.Y.; Diao, N.R.; Fang, Z.H. A finite line- source model for boreholes in geothermal heat exchangers. *Heat Transf. Res. Co-sponsored by Soc. Chem. Eng. Japan Heat Transf. Div. ASME* **2002**, *31*, 558–567.

16. Lamarche, L.; Beauchamp, B. New solutions for the short-time analysis of geothermal vertical boreholes. *Int. J. Heat Mass Transf.* **2007**, *50*, 1408–1419, doi:10.1016/J.IJHEATMASSTRANSFER.2006.09.007.

17. Lamarche, L. A fast algorithm for the hourly simulations of ground-source heat pumps using arbitrary response factors. *Renew. Energy* **2009**, *34*, 2252–2258, doi:10.1016/j.renene.2009.02.010.

18. Marcotte, D.; Pasquier, P. Fast fluid and ground temperature computation for geothermal ground-loop heat exchanger systems. *Geothermics* **2008**, *37*, 651–665, doi:10.1016/j.geothermics.2008.08.003.

19. Cimmino, M.; Bernier, M. A semi-analytical method to generate g-functions for geothermal bore fields. *Int. J. Heat Mass Transf.* **2014**, *70*, 641–650, doi:10.1016/j.ijheatmasstransfer.2013.11.037.

20. Lamarche, L. Mixed arrangement of multiple input-output borehole systems. *Appl. Therm. Eng.* **2017**, *124*, 466–476, doi:10.1016/j.applthermaleng.2017.06.060.

21. Bandos, T. V; Montero, A.; Fernandez, E.; Santander, J.L.G.; Isidro, J.M.; Perez, J.; de Cordoba, P.J.F.; Urchueguia, J.F. Finite line-source model for borehole heat exchangers: effect of vertical temperature variations. *Geothermics* **2009**, *38*, 263–270, doi:10.1016/j.geothermics.2009.01.003.

22. Molina-Giraldo, N.; Blum, P.; Zhu, K.; Bayer, P.; Fang, Z.H. A moving finite line source model to simulate borehole heat exchangers with

groundwater advection. *Int. J. Therm. Sci.* **2011**, *50*, 2506–2513, doi:10.1016/j.ijthermalsci.2011.06.012.

23. Eskilson, P. Thermal analysis of heat extraction boreholes, Lund Inst. of Tech. (Sweden). Dept. of Mathematical Physics: Lund, Sweden, 1987.

24. Priarone, A.; Fossa, M. Temperature response factors at different boundary conditions for modelling the single borehole heat exchanger. *Appl. Therm. Eng.* **2016**, *103*, 934–944, doi:10.1016/j.applthermaleng.2016.04.038.

25. Monzó, P. Modelling and monitoring thermal response of the ground in borehole fields, Kungliga Tekniska högskolan: Stockholm, Sweden, 2018.

26. Naldi, C.; Zanchini, E. A new numerical method to determine isothermal g-functions of borehole heat exchanger fields. *Geothermics* **2019**, *77*, 278–287.

27. Belzile, P.; Lamarche, L.; Rousse, D.R. Semi-analytical model for geothermal borefields with independent inlet conditions. *Geothermics* **2016**, *60*, 144–155, doi:10.1016/j.geothermics.2015.12.008.

28. Yavuzturk, C.; Spitler, J.D. A short time step response factor model for vertical ground loop heat exchangers. *Ashrae Trans.* **1999**, *105*, 475–485.

29. Naldi, C.; Zanchini, E. A one-material cylindrical model to determine short-and long-term fluid-to-ground response factors of single U-tube borehole heat exchangers. *Geothermics* **2020**, *86*, 101811.

30. Yu, X.; Li, H.; Yao, S.; Nielsen, V.; Heller, A. Development of an efficient numerical model and analysis of heat transfer performance for borehole heat exchanger. *Renew. Energy* **2020**, *152*, 189–197.

31. Hellström, G. Ground heat storage thermal analysis of duct storage systems. Part I. Theory. *Sweden PhD. thesis, Univ. Lund* **1991**.

32. Zarrella, A.; Scarpa, M.; De Carli, M. Short time step analysis of vertical ground-coupled heat exchangers: The approach of CaRM. *Renew. Energy* **2011**, *36*, 2357–2367, doi:https://doi.org/10.1016/j.renene.2011.01.032.

33. Pasquier, P.; Marcotte, D. Short-term simulation of ground heat exchanger with an improved TRCM. *Renew. Energy* **2012**, *46*, 92–99, doi:10.1016/J.RENENE.2012.03.014.

34. Javed, S.; Claesson, J. New Analytical and Numerical Solutions for the Short-term Analysis of Vertical Ground Heat Exchangers. *Ashrae Trans. 2011, Vol 117, Pt 1* **2011**, *117*, 3–12.

35. De Rosa, M.; Ruiz-Calvo, F.; Corberán, J.M.; Montagud, C.; Tagliafico, L.A. A novel TRNSYS type for short-term borehole heat exchanger simulation: B2G model. *Energy Convers. Manag.* **2015**, *100*, 347–357, doi:https://doi.org/10.1016/j.enconman.2015.05.021.

36. Young, T.R. Development, verification, and design analysis of the borehole fluid thermal mass model for approximating short term borehole thermal response 2004.

37. Lamarche, L. Short-time analysis of vertical boreholes, new analytic solutions and choice of equivalent radius. *Int. J. Heat Mass Transf.* **2015**, *91*, 800–807, doi:https://doi.org/10.1016/j.ijheatmasstransfer.2015.07.135.

38. Li, M.; Lai, A.C.K. New temperature response functions (G functions) for pile and borehole ground heat exchangers based on composite-medium line-source theory. *Energy* **2012**, *38*, 255–263, doi:10.1016/J.ENERGY.2011.12.004.

39. Rivero, J.M.; Hermanns, M. Enhanced multipole method for the transient thermal response of slender geothermal boreholes. *Int. J. Therm. Sci.* **2021**, *164*, 106531.

40. Prieto, C.; Cimmino, M. Transient multipole expansion for heat transfer in ground heat exchangers. *Sci. Technol. Built Environ.* **2020**, *27*, 253–270.

41. Rees, S.J.; He, M.M. A three-dimensional numerical model of borehole heat exchanger heat transfer and fluid flow. *Geothermics* **2013**, *46*, 1–13, doi:10.1016/j.geothermics.2012.10.004.

42. Ruiz-Calvo, F.; De Rosa, M.; Monzó, P.; Montagud, C.; Corberán, J.M. Coupling short-term (B2G model) and long-term (g-function) models for ground source heat exchanger simulation in TRNSYS. Application in a real installation. *Appl. Therm. Eng.* **2016**, *102*, 720–732, doi:https://doi.org/10.1016/j.applthermaleng.2016.03.127.

43. Figueroa, I.C.; Cimmino, M.; Helsen, L. A Methodology for Long-Term Model Predictive Control of Hybrid Geothermal Systems: The Shadow-Cost Formulation. *Energies* **2020**, *13*.

44. Huang, J.; Fan, J.; Furbo, S. Demonstration and optimization of a solar district heating system with ground source heat pumps. *Sol. Energy* **2020**, *202*, 171–189.

45. Miglani, S.; Orehounig, K.; Carmeliet, J. Integrating a thermal model of ground source heat pumps and solar regeneration within building energy

system optimization. *Appl. Energy* **2018**, *218*, 78–94.

46. Ikeda, S.; Choi, W.; Ooka, R. Optimization method for multiple heat source operation including ground source heat pump considering dynamic variation in ground temperature. *Appl. Energy* **2017**, *193*, 466–478.

47. Reda, F. Long term performance of different SAGSHP solutions for residential energy supply in Finland. *Appl. Energy* **2015**, *144*, 31–50.

48. Nouri, G.; Noorollahi, Y.; Yousefi, H. Designing and optimization of solar assisted ground source heat pump system to supply heating, cooling and hot water demands. *Geothermics* **2019**, *82*, 212–231.

49. Zhang, X.; Li, H.; Liu, L.; Bai, C.; Wang, S.; Song, Q.; Zeng, J.; Liu, X.; Zhang, G. Optimization analysis of a novel combined heating and power system based on biomass partial gasification and ground source heat pump. *Energy Convers. Manag.* **2018**, *163*, 355–370.

50. Zeng, R.; Li, H.; Jiang, R.; Liu, L.; Zhang, G. A novel multi-objective optimization method for CCHP–GSHP coupling systems. *Energy Build.* **2016**, *112*, 149–158.

51. Mogensen, P. Fluid to duct wall heat transfer in duct system heat storages. *Doc. Counc. Build. Res.* **1983**, 652–657.

52. Gehlin, S. Thermal response test: in situ measurements of thermal properties in hard rock, Luleå tekniska universitet: Luleå, Sweden, 1998.

53. Witte, H.J.L. Error analysis of thermal response tests. *Appl. Energy* **2013**, *109*, 302–311, doi:10.1016/j.apenergy.2012.11.060.

54. Hellström, G.; Sanner, B.; Klugescheid, M.; Gonka, T.; Mårtensson, S. Experiences with the borehole heat exchanger software EED. *Proc. Megastock* **1997**, *97*, 247–252.

55. Ruiz-Calvo, F.; Cervera-Vazquez, J.; Montagud, C.; Corberan, J.M. Reference data sets for validating and analyzing GSHP systems based on an eleven-year operation period. *Geothermics* **2016**, *64*, 538–550, doi:10.1016/j.geothermics.2016.08.004.

56. Naiker, S.S.; Rees, S.J. Monitoring and performance analysis of a large non-domestic ground source heat pump installation.; CIBSE, 2011.

57. Kim, S.-K.; Bae, G.-O.; Lee, K.-K.; Song, Y. Field-scale evaluation of the design of borehole heat exchangers for the use of shallow geothermal energy. *Energy* **2010**, *35*, 491–500.

58. Tordrup, K.W.; Poulsen, S.E.; Bjorn, H. An improved method for upscaling borehole thermal energy storage using inverse finite element modelling. *Renew. Energy* **2017**, *105*, 13–21, doi:10.1016/j.renene.2016.12.011.

59. Fernandez, M.; Eguia, P.; Granada, E.; Febrero, L. Sensitivity analysis of a vertical geothermal heat exchanger dynamic simulation: Calibration and error determination. *Geothermics* **2017**, *70*, 249–259, doi:10.1016/j.geothermics.2017.06.012.

60. Esen, H.; Inalli, M. Modelling of a vertical ground coupled heat pump system by using artificial neural networks. *Expert Syst. Appl.* **2009**, *36*, 10229–10238.

61. Sun, W.; Hu, P.; Lei, F.; Zhu, N.; Jiang, Z. Case study of performance evaluation of ground source heat pump system based on ANN and ANFIS models. *Appl. Therm. Eng.* **2015**, *87*, 586–594.

62. Pasquier, P.; Zarrella, A.; Labib, R. Application of artificial neural networks to near-instant construction of short-term g-functions. *Appl. Therm. Eng.* **2018**, *143*, 910–921, doi:10.1016/j.applthermaleng.2018.07.137.

63. Gang, W.; Wang, J. Predictive ANN models of ground heat exchanger for the control of hybrid ground source heat pump systems. *Appl. Energy* **2013**, *112*, 1146–1153.

64. Lee, D.; Ooka, R.; Ikeda, S.; Choi, W. Artificial neural network prediction models of stratified thermal energy storage system and borehole heat exchanger for model predictive control. *Sci. Technol. Built Environ.* **2019**, *25*, 534–548.

65. Underwood, C. On the design and response of domestic ground-source heat pumps in the UK. *Energies* **2014**, *7*, 4532–4553.

66. Shu, H.; Duanmu, L.; Shi, J.; Jia, X.; Ren, Z.; Yu, H. Field measurement and energy efficiency enhancement potential of a seawater source heat pump district heating system. *Energy Build.* **2015**, *105*, 352–357.

67. Afjei, T.; Wetter, M. Compressor heat pump including frost and cycle losses. *Model Descr. Implement. into TRNSYS, Ingenieurschule HTL* **1997**.

68. Lee, T.-S.; Lu, W.-C. An evaluation of empirically-based models for predicting energy performance of vapor-compression water chillers. *Appl. Energy* **2010**, *87*, 3486–3493.

69. Swider, D.J. A comparison of empirically based steady-state models for vapor-compression liquid chillers. *Appl. Therm. Eng.* **2003**, *23*, 539–556, doi:https://doi.org/10.1016/S1359-4311(02)00242-9.

70. Bechtler, H.; Browne, M.W.; Bansal, P.K.; Kecman, V. Neural networks—a new approach to model vapour- compression heat pumps. *Int. J. Energy Res.* **2001**, *25*, 591–599.

71. Arcaklioğlu, E.; Erişen, A.; Yilmaz, R. Artificial neural network analysis of heat pumps using refrigerant mixtures. *Energy Convers. Manag.* **2004**, *45*, 1917–1929.

72. Zhang, Y.; Cui, C.; Yuan, J.; Zhang, C.; Gang, W. Quantification of model uncertainty of water source heat pump and impacts on energy performance. In Proceedings of the IOP Conference Series: Earth and Environmental Science; IOP Publishing, 2019; Vol. 238, p. 12067.

73. Carbonell Sánchez, D.; Cadafalch Rabasa, J.; Pärlisch, P.; Consul Serracanta, R. Numerical analysis of heat pumps models: comparative study between equation-fit and refrigerant cycle based models. In Proceedings of the Solar energy for a brighter future: book of proceedings: EuroSun 2012; 2012.

74. Lucia, U.; Simonetti, M.; Chiesa, G.; Grisolia, G. Ground-source pump system for heating and cooling: Review and thermodynamic approach. *Renew. Sustain. Energy Rev.* **2017**, *70*, 867–874.

75. Aresti, L.; Christodoulides, P.; Florides, G. A review of the design aspects of ground heat exchangers. *Renew. Sustain. Energy Rev.* **2018**, *92*, 757–773.

76. Sanner, B. Ground Source Heat Pumps–history, development, current status, and future prospects. In Proceedings of the Proceedings of 12th IEA Heat Pump Conference (paper K. 2.9.).; Rotterdam, 2017; pp. 1–14.

77. Dehghan, B.; Wang, L.; Motta, M.; Karimi, N. Modelling of waste heat recovery of a biomass combustion plant through ground source heat pumps-development of an efficient numerical framework. *Appl. Therm. Eng.* **2020**, *166*, 114625.

78. Kang, S.; Li, H.; Lei, J.; Liu, L.; Cai, B.; Zhang, G. A new utilization approach of the waste heat with mid-low temperature in the combined heating and power system integrating heat pump. *Appl. Energy* **2015**, *160*, 185–193.

79. Nouri, G.; Noorollahi, Y.; Yousefi, H. Solar assisted ground source heat pump systems–A review. *Appl. Therm. Eng.* **2019**, *163*, 114351.

80. Monzo, P.; Mogensen, P.; Acuna, J.; Ruiz-Calvo, F.; Montagud, C. A novel numerical approach for imposing a temperature boundary condition at the borehole wall in borehole fields. *Geothermics* **2015**, *56*, 35–44, doi:10.1016/j.geothermics.2015.03.003.

81. Cimmino, M.; Bernier, M.; Adams, F. A contribution towards the determination of g-functions using the finite line source. *Appl. Therm. Eng.* **2013**, *51*, 401–412.

82. Hellström, G.; Sanner, B. Software for dimensioning of deep boreholes for heat extraction. *Proc. Calorstock* **1994**, *94*, 195–202.

83. Spitler, J.D. GLHEPRO-A design tool for commercial building ground loop heat exchangers. In Proceedings of the Proceedings of the fourth international heat pumps in cold climates conference; Citeseer, 2000.

84. Monzó, P.; Puttige, A.R.; Acuña, J.; Mogensen, P.; Cazorla, A.; Rodriguez, J.; Montagud, C.; Cerdeira, F. Numerical modeling of ground thermal response with borehole heat exchangers connected in parallel. *Energy Build.* **2018**, *172*, doi:10.1016/j.enbuild.2018.04.057.

85. Al-Khoury, R.; Kölbel, T.; Schramedei, R. Efficient numerical modeling of borehole heat exchangers. *Comput. Geosci.* **2010**, *36*, 1301–1315.

86. Lee, C.K.; Lam, H.N. A modified multi-ground-layer model for borehole ground heat exchangers with an inhomogeneous groundwater flow. *Energy* **2012**, *47*, 378–387.

87. Luo, J.; Rohn, J.; Bayer, M.; Priess, A.; Xiang, W. Analysis on performance of borehole heat exchanger in a layered subsurface. *Appl. Energy* **2014**, *123*, 55–65.

88. Yang, H.; Cui, P.; Fang, Z. Vertical-borehole ground-coupled heat pumps: A review of models and systems. *Appl. Energy* **2010**, *87*, 16–27, doi:https://doi.org/10.1016/j.apenergy.2009.04.038.

89. Lamarche, L.; Beauchamp, B. A new contribution to the finite line-source model for geothermal boreholes. *Energy Build.* **2007**, *39*, 188–198, doi:10.1016/j.enbuild.2006.06.003.

90. Lazzarotto, A. A network-based methodology for the simulation of borehole heat storage systems. *Renew. Energy* **2014**, *62*, 265–275, doi:10.1016/j.renene.2013.07.020.

91. Marcotte, D.; Pasquier, P. Unit-response function for ground heat exchanger with parallel, series or mixed borehole arrangement. *Renew. Energy* **2014**, *68*, 14–24, doi:10.1016/j.renene.2014.01.023.

92. Cimmino, M. A finite line source simulation model for geothermal systems with series- and parallel-connected boreholes and independent fluid loops. *J. Build. Perform. Simul.* **2018**, *11*, 414–432, doi:10.1080/19401493.2017.1381993.

93. Lazzarotto, A.; Björk, F. A methodology for the calculation of response functions for geothermal fields with arbitrarily oriented boreholes–Part 2. *Renew. energy* **2016**, *86*, 1353–1361.

94. Abdelaziz, S.L.; Ozudogru, T.Y.; Olgun, C.G.; Martin II, J.R. Multilayer finite line source model for vertical heat exchangers. *Geothermics* **2014**, *51*, 406–416.

95. Yavuzturk, C.; Spitler, J.D. Field validation of a short time step model for vertical ground-loop heat exchangers/Discussion. *ASHRAE Trans.* **2001**, *107*, 617.

96. Bauer, D.; Heidemann, W.; Müller-Steinhagen, H.; Diersch, H.-J.G. Thermal resistance and capacity models for borehole heat exchangers. *Int. J. Energy Res.* **2011**, *35*, 312–320, doi:10.1002/er.1689.

97. Cazorla-Marín, A.; Montagud-Montalvá, C.; Tinti, F.; Corberán, J.M. A novel TRNSYS type of a coaxial borehole heat exchanger for both short and mid term simulations: B2G model. *Appl. Therm. Eng.* **2020**, *164*, 114500.

98. Wei, J.; Wang, L.; Jia, L.; Zhu, K.; Diao, N. A new analytical model for short-time response of vertical ground heat exchangers using equivalent diameter method. *Energy Build.* **2016**, *119*, 13–19, doi:https://doi.org/10.1016/j.enbuild.2016.02.055.

99. Xu, X.; Spitler, J.D. Modeling of vertical ground loop heat exchangers with variable convective resistance and thermal mass of the fluid. In Proceedings of the Proceedings of the 10th International Conference on Thermal Energy Storage. Ecostock; 2006.

100. Gustafsson, A.-M.; Gehlin, S. Influence of natural convection in water-filled boreholes for GCHP. In Proceedings of the ASHRAE Transactions; 2008; Vol. 114 PART 1, pp. 416–423.

101. Kjellsson, E.; Hellström, G. Laboratory study of the heat transfer in a water-filled borehole with a single U-pipe. In Proceedings of the Megastock 1997 The 7th international conference on thermal energy storage. Sapporo, Japan; 1997; pp. 509–514.

102. Gustafsson, A.-M.; Westerlund, L. Multi-injection rate thermal response test in groundwater filled borehole heat exchanger. *Renew. Energy* **2010**,

35, 1061–1070, doi:https://doi.org/10.1016/j.renene.2009.09.012.

103. Spitler, J.D.; Javed, S.; Ramstad, R.K. Natural convection in groundwater-filled boreholes used as ground heat exchangers. *Appl. Energy* **2016**, *164*, 352–365.

104. Johnsson, J.; Adl-Zarrabi, B. Modelling and evaluation of groundwater filled boreholes subjected to natural convection. *Appl. Energy* **2019**, *253*, 113555.

105. Florides, G.A.; Christodoulides, P.; Pouloupatis, P. An analysis of heat flow through a borehole heat exchanger validated model. *Appl. Energy* **2012**, *92*, 523–533, doi:10.1016/j.apenergy.2011.11.064.

106. Esen, H.; Inalli, M.; Esen, Y. Temperature distributions in boreholes of a vertical ground-coupled heat pump system. *Renew. Energy* **2009**, *34*, 2672–2679, doi:https://doi.org/10.1016/j.renene.2009.04.032.

107. Lee, C.K.; Lam, H.N. Computer simulation of borehole ground heat exchangers for geothermal heat pump systems. *Renew. Energy* **2008**, *33*, 1286–1296, doi:https://doi.org/10.1016/j.renene.2007.07.006.

108. Underwood, C.P. 14 - Heat pump modelling. In; Rees, S.J.B.T.-A. in G.-S.H.P.S., Ed.; Woodhead Publishing, 2016; pp. 387–421 ISBN 978-0-08-100311-4.

109. Sami, S.M.; Dahmani, A. Numerical prediction of dynamic performance of vapour-compression heat pump using new HFC alternatives to HCFC-22. *Appl. Therm. Eng.* **1996**, *16*, 691–705, doi:https://doi.org/10.1016/1359-4311(95)00075-5.

110. Koury, R.N.N.; Machado, L.; Ismail, K.A.R. Numerical simulation of a variable speed refrigeration system. *Int. J. Refrig.* **2001**, *24*, 192–200, doi:https://doi.org/10.1016/S0140-7007(00)00014-1.

111. Browne, M.W.; Bansal, P.K. Transient simulation of vapour-compression packaged liquid chillers. *Int. J. Refrig.* **2002**, *25*, 597–610, doi:https://doi.org/10.1016/S0140-7007(01)00060-3.

112. Corberán, J.M.; Gonzálvez, J.; Montes, P.; Blasco, R. 'ART'a computer code to assist the design of refrigeration and A/C equipment. **2002**.

113. Cimmino, M.; Wetter, M. Modelling of heat pumps with calibrated parameters based on manufacturer data. In Proceedings of the Proceedings of the 12th International Modelica Conference, Prague, Czech Republic, May 15-17, 2017; 2017; pp. 219–226.

114. Jin, H. Parameter estimation based models of water source heat pumps 2002.

115. Swider, D.J.; Browne, M.W.; Bansal, P.K.; Kecman, V. Modelling of vapour-compression liquid chillers with neural networks. *Appl. Therm. Eng.* **2001**, *21*, 311–329.

116. Baik, Y.-J.; Kim, M.; Chang, K.-C.; Lee, Y.-S.; Ra, H.-S. Potential to enhance performance of seawater-source heat pump by series operation. *Renew. Energy* **2014**, *65*, 236–244, doi:https://doi.org/10.1016/j.renene.2013.09.021.

117. Ruschenburg, J.; Ćutić, T.; Herkel, S. Validation of a black-box heat pump simulation model by means of field test results from five installations. *Energy Build.* **2014**, *84*, 506–515.

118. Yang, K.-T. Artificial neural networks (ANNs): a new paradigm for thermal science and engineering. *J. Heat Transfer* **2008**, *130*.

119. Hochreiter, S.; Schmidhuber, J. Long Short-Term Memory. *Neural Comput.* **1997**, *9*, 1735–1780, doi:10.1162/neco.1997.9.8.1735.

120. Cho, K.; Van Merriënboer, B.; Gulcehre, C.; Bahdanau, D.; Bougares, F.; Schwenk, H.; Bengio, Y. Learning phrase representations using RNN encoder-decoder for statistical machine translation. *arXiv Prepr. arXiv1406.1078* **2014**.

121. Mohanraj, M.; Jayaraj, S.; Muraleedharan, C. Applications of artificial neural networks for refrigeration, air-conditioning and heat pump systems—a review. *Renew. Sustain. energy Rev.* **2012**, *16*, 1340–1358.

122. Zhou, S.; Liu, D.; Cao, S.; Liu, X.; Zhou, Y. An application status review of computational intelligence algorithm in GSHP field. *Energy Build.* **2019**, *203*, 109424, doi:https://doi.org/10.1016/j.enbuild.2019.109424.

123. Esen, H.; Inalli, M.; Sengur, A.; Esen, M. Performance prediction of a ground-coupled heat pump system using artificial neural networks. *Expert Syst. Appl.* **2008**, *35*, 1940–1948, doi:10.1016/j.eswa.2007.08.081.

124. Fannou, J.-L.C.; Rousseau, C.; Lamarche, L.; Kajl, S. Modeling of a direct expansion geothermal heat pump using artificial neural networks. *Energy Build.* **2014**, *81*, 381–390.

125. Park, S.K.; Moon, H.J.; Min, K.C.; Hwang, C.; Kim, S. Application of a multiple linear regression and an artificial neural network model for the heating performance analysis and hourly prediction of a large-scale

ground source heat pump system. *Energy Build.* **2018**, *165*, 206–215, doi:https://doi.org/10.1016/j.enbuild.2018.01.029.

126. Chen, S.; Mao, J.; Chen, F.; Hou, P.; Li, Y. Development of ANN model for depth prediction of vertical ground heat exchanger. *Int. J. Heat Mass Transf.* **2018**, *117*, 617–626.

127. Arat, H.; Arslan, O. Optimization of district heating system aided by geothermal heat pump: A novel multistage with multilevel ANN modelling. *Appl. Therm. Eng.* **2017**, *111*, 608–623.

128. Kalogirou, S.A.; Florides, G.A.; Pouloupatis, P.D.; Christodoulides, P.; Joseph-Stylianou, J. Artificial neural networks for the generation of a conductivity map of the ground. *Renew. Energy* **2015**, *77*, 400–407, doi:https://doi.org/10.1016/j.renene.2014.12.033.

129. Zhang, Y.; Zhou, L.; Hu, Z.; Yu, Z.; Hao, S.; Lei, Z.; Xie, Y. Prediction of layered thermal conductivity using artificial neural network in order to have better design of ground source heat pump system. *Energies* **2018**, *11*, 1896.

130. Dusseault, B.; Pasquier, P. Efficient g-function approximation with artificial neural networks for a varying number of boreholes on a regular or irregular layout. *Sci. Technol. Built Environ.* **2019**, *25*, 1023–1035.

131. Sayyadi, H.; Nejatolahi, M. Thermodynamic and thermoeconomic optimization of a cooling tower-assisted ground source heat pump. *Geothermics* **2011**, *40*, 221–232.

132. Sivasakthivel, T.; Murugesan, K.; Thomas, H.R. Optimization of operating parameters of ground source heat pump system for space heating and cooling by Taguchi method and utility concept. *Appl. Energy* **2014**, *116*, 76–85.

133. Ma, W.; Fang, S.; Liu, G. Hybrid optimization method and seasonal operation strategy for distributed energy system integrating CCHP, photovoltaic and ground source heat pump. *Energy* **2017**, *141*, 1439–1455.

134. Li, W.; Li, X.; Wang, Y.; Tu, J. An integrated predictive model of the long-term performance of ground source heat pump (GSHP) systems. *Energy Build.* **2018**, *159*, 309–318.

135. Ruiz-Calvo, F.; Montagud, C.; Cazorla-Marín, A.; Corberán, J.M. Development and experimental validation of a TRNSYS dynamic tool for design and energy optimization of ground source heat pump systems. *Energies* **2017**, *10*, 1510.

136. Wetter, M. Genopt R, generic optimization program, user manual, version 3.1. 1. lawrence berkeley national laboratory; 2016. *Man. Progr. downloadable Free Charg. from, http//simulationresearch. lbl. gov/GO/(last accessed 10.08. 13)*.

137. Cimmino, M. The effects of borehole thermal resistances and fluid flow rate on the g-functions of geothermal bore fields. *Int. J. Heat Mass Transf.* **2015**, *91*, 1119–1127.

138. Ruiz-Calvo, F.; Montagud, C. Reference data sets for validating GSHP system models and analyzing performance parameters based on a five-year operation period. *Geothermics* **2014**, *51*, 417–428, doi:10.1016/j.geothermics.2014.03.010.